Department of Chemical, Materials and Industrial Production Engineering

XXXVII Cycle

Thesis for the Degree of Doctor of Philosophy

Design and Fabrication of Polymeric Composite Platforms Using Electro-Fluid Dynamic Techniques for Biomedical Applications

Supervisors:

Vincenzo Guarino (CNR)

Sergio Caserta (UNINA)

PhD Candidate:

Nergis Zeynep RENKLER DEGIRMENCI

Contents

ABSTRACT

Over the last two decades, electro-fluid dynamic techniques (EFDT), including electrospinning and electrospraying, have been established as general methods for the synthesis and processing of micro- and nano-structured materials. These methods allow working with certain polymers of both natural and synthetic origin giving a novel possibility of engineering new generation materials for medical needs. Due to the ability to customize such material features as fiber shape, available area, and tensile strength, EFDT is regarded as a crucial means for a wide range of new applications in tissue engineering, drug delivery, and biosensing.

This thesis investigates the potential of EFDT for the fabrication of advanced polymeric composite platforms and their use in biomedical areas. The research primarily focuses on the use of electrospinning and electrospraying for creating nanofibers and microgels with specific properties for tissue engineering, drug delivery, and biosensing applications. The study displays the enhancements of properties of Polyvinyl Alcohol (PVA) as a material starting point and by modifying of its compositions e.g. by blending it with natural polymers such as gelatin and by complexation with MXenes. PVA was selected due to its excellent biocompatibility, water solubility, and film-forming properties, which make it an ideal candidate for biomedical applications. Structural, mechanical and functional properties of the fabricated nano fibrous scaffolds were able to enhance cell adhesion, proliferation and bioactivity. Moreover, electro-sprayed core-shell alginate microspheres exhibited sustained release characteristics and targeted drug delivery with adjustable release kinetics depending on shell thickness and macromolecular structure.

The thesis proposes creating biomedical materials in a more sustainable way by utilizing aqueous-based electrospinning and green crosslinking. These environmentally friendly approaches tackle problems like reproducibility, scalability and biocompatibility within the context of biomedical material fabrication. The results support the development of

advanced biomaterials targeted for the era of personalized medicine, precision drug delivery systems and regenerative therapies.

Keywords: Electrospinning; Electrospraying; Nanofibers; Nanoparticles; Biomaterials

LIST OF ABBREVIATIONS

The following abbreviations are used throughout the thesis.

3D: Three-Dimensional

AQP-4: Aquaporin 4

ANOVA: Analysis of Variance

CNS: Central Nervous System

CNTs: Carbon Nanotubes

DicNa: Diclofenac Sodium

DMEM: Dulbecco's Modified Eagle Medium

DSC: Differential Scanning Calorimetry

EDC: 1-Ethyl-3-(3-dimethylaminopropyl) Carbodiimide

EFDT: Electro-Fluid Dynamic Techniques

ECM: Extracellular Matrix

EDS: Energy Dispersive X-Ray Spectroscopy

F-Actin: Filamentous Actin

FE-SEM: Field-Emission Scanning Electron Microscope

FBS: Fetal Bovine Serum

FTIC: Fluorescein Isothiocyanate

FTIR: Fourier-Transform Infrared Spectroscopy

GEL: Gelatin

GFAP: Glial Fibrillary Acidic Protein

GO: Graphene Oxide

HA: Hydroxyapatite

HFIP: Hexafluoroisopropanol

HV: High Viscosity

LV: Low Viscosity

NHS: N-Hydroxy Succinimide

PCL: Polycaprolactone

PBS: Phosphate-Buffered Saline

PdL: Poly-D-Lysine

PEO: Polyethylene Oxide

PLA: Poly(lactic acid)

PVA: Poly(vinyl alcohol)

RGD: Arginine-Glycine-Aspartic Acid (a cell adhesive motif in proteins)

SA: Sodium Alginate

SEM: Scanning Electron Microscope

TFE: Trifluoroethanol

TGA: Thermogravimetric Analysis

WAXS: Wide Angle X-ray Scattering

XTT: Cell Proliferation Kit Assay

LIST OF FIGURES

INTRODUCTION

Nowadays, it is common to see numerous biomaterials – from many synthetic or natural sources – being continually fabricated with an intensified precision in their structural features. This enables them to be able to be made into three-dimensional (3D) architectures that are suitable for tissue engineering and other therapeutic interventions. While the constituent materials inclusive of their physical/chemical characteristics remain of interest, it is well known that peculiar structural features at different scales of these products can have a significant impact on the eventual properties of these products. For example, a number of research papers have shown that the use of nano- or microparticles in injection applications is ideal than using particles which are hundreds of microns or millimeters large [1]. Similarly, in the case of fibrous scaffolds used in vitro, nano-textured surfaces, i.e., fiber diameters at the nanoscale, better mimic the architecture of basement lamina membranes found in natural tissues, thereby enhancing biomechanical and biological interactions such as cell adhesion, proliferation, and fluid/molecular transport properties [2]. In some medical solutions that involve bio-filtration processes, nanofibrous membranes help to eliminate medical bio-contaminants and thus enhance the separation efficiency of the membranes through improved flux and reduced energy consumption [3]. Therefore, it is necessary to apply such advanced processing technologies that are capable of maintaining desired micro- and nano-scale structural characteristics. Such level of precision makes it possible to fabricate materials that possess specific morphological and topographical features for targeted biomedical applications[4]. EFDT including electrospinning and electrospraying have gained wide spread application among micro and nanostructured materials for being simple and low cost approaches. This enables the creation of fibers or particles with specified dimensions and properties by utilizing high-voltage electric fields to guide polymeric solutions or melts. The broad use of polymers and composites with EFDT has revolutionized tissue engineering, drug delivery, biosensing and other medical fields [5], [6].

This thesis investigates the potential of EFDT for the fabrication of polymeric composite platforms designed for biomedical applications. By integrating suitable synthetic polymers like Polyvinyl Alcohol (PVA) with natural polymers such as gelatin and advanced materials like MXenes, the work presented here addresses key challenges such as biocompatibility, mechanical stability, and scalability. Additionally, the incorporation of environmentally friendly fabrication methods, such as aqueous-based electrospinning and green crosslinking, reflects the growing demand for sustainable approaches in biomaterials development.

The structure of the thesis is as follows:

- Chapter 1 introduces the major concepts of EFDT, namely the electrospinning and electrospraying processes, and provides an overview of their applications in the biomedical field. It further deals with the problems and prospects in the development of polymeric materials for certain uses. Related to this chapter, the author's publication [7] can be found, which further elaborate on the subject .
- Chapter 2 focuses on multicomponent polymeric platforms reaching to a depth of the commonly used materials, their characteristics and the designs needed for particular biomedical applications. Related to this chapter, the author's publication [8] can be found, which further elaborate on the subject.
- Chapter 3 describes the preparation and optimization of PVA-based nanofibers, and further highlights solution parameters, process conditions and post-processing treatments as the factors that affect the final properties of the material. Related to this chapter, the author's publication [9]can be found, which further elaborate on the subject.
- Chapter 4 explores the preparation of bioactive nanofibers scaffolds where PVA was blended with gelatin to fabricate scaffolds that improve cell responses and tissue regeneration.
- Chapter 5 investigates the creation of electroactive nanofibers by MXenes and other conductive materials. These materials are being investigated for the potential of nerve and muscle tissue engineering as well as biosensor applications. Related to this chapter, the author's publication can be found [10], which further elaborate on the subject.

- Chapter 6 examines to the use of EFDT in drug delivery systems where both the nanofibers and the microgels are shown as the devices for making available the therapeutic agents at the desirable site and at regulated rates. Related to part of this chapter, the author's involved publication can be found [11], which further elaborate on the subject.
- Chapter 7 concludes the thesis by summarizing the findings, discussing their implications for biomedical engineering, and proposing future research directions.

This thesis proposes an integrated framework in the engineering and development of polymeric systems using EFDT, addressing the pressing issues of scale up, bio-integration and functionality. By sequentially merging newer materials and greener processes, The goal is to foster the development of next generation biomaterials for application in regenerative medicine and personalized therapies.

Chapter 1

1. ELECTRO-FLUID DYNAMIC TECHNOLOGIES

Electro-fluid dynamics refers to the interaction of electrical forces with fluids, whether liquids or gases. EFDT has established itself as an energy-efficient, highly versatile, and effective tool to influence fluids [12]. They include two different working modes, electrospinning and electrospraying, that allow producing, respectively, non-woven fibers or particles of different sizes and shapes. They are highly tunable in their characteristic size and shape by accurately selecting the materials/solvents/additives and finely controlling the process parameters [13]. Moreover, many materials, such as synthetic and natural polymers, metals, ceramics, composites, and blend systems can be sagely combined for the fabrication of multicomponent devices suitable in many fields such as tissue engineering and regenerative medicine [14], drug delivery [15], wound dressing [16], bioelectronics [17], and biofiltration systems [18].

Despite the recent goals in terms of research outcomes in the biomedical field, upscaling EFDT for clinical translation and large-scale production is still so far due to several problems concerning the current biomanufacturing processes, mainly related to the use of volatile solvents and all the risk factors connected to health and safety standards during fabrication and product implementation [19].

It is well known that the solvent evaporation mechanism drives conventional electrospinning. Environmental damage associated with using organic solvents with low boiling points—namely Trifluoroethanol (TFE) and dichloromethane (DCM)—may not be thoroughly recommended by the U.S. Food and Drug Administration for the fabrication of electrospun fibers for pharmaceutical applications. Moreover, solvent traces may be

entrapped into the fiber body after resting treatments, thus restricting their use for biological use that requires direct contact with the cells [20].

In this chapter, an overview of the different EFDTs was proposed. In the first part, working principles were introduced, highlighting some recently explored insights to minimize the manufacturing impact on the environment (i.e., melt electrospinning, green electrospinning). In the second part, a wide range of blends or composite devices based on fibers or particles with different size scales were systematically discussed according to their application in the biomedical and environmental fields.

1.1. Classification and Basic Principles of EFDTs

EFDTs can be considered a class of "bottom-up" technologies that use high-voltage electric forces on viscoelastic polymers at the melt state or in solution form. It includes two main processing modes: electrically assisted spinning and spraying—suitable to synthesize micro- and nanostructures in the form of particles or fibers [5]. Their popularity is mainly due to the high reliability and versatility of these processes that allow fabricating a plethora of smart devices with controlled sizes from micro- to submicrometric scale and multiple functionalities as a function of the specific experimental configuration used.

The most elementary configuration is straightforward and includes three components: a high-voltage power supply, a pump system where a syringe/cartridge is arranged, and a ground collector. Polymer comes out of the needle tip at a constant rate with the support of pumping forces until a droplet is formed [21]. Two opposite forces contribute to forming the droplet: the electrostatic force acting on this droplet shape and the opposite force, the surface tension force, that tends to preserve the droplet's spherical shape. At the point that the two forces have equilibrium, it is expressed by the following equation:

$$\frac{1}{8\rho\varepsilon o}.\frac{Q2}{R2} = 8\rho\sigma sR$$

where Q is the charge located on the droplet surface, R is the droplet radius, εo is the vacuum permeability, and σs is the surface tension coefficient. The charge increases by

increasing the strength of the electric field, and the value of this electrostatic field force can be controlled by varying the voltage at a fixed distance between the two electrodes [22]. Up to a critical point where the electrostatic force overcomes the surface tension, the droplet is then disrupted into smaller droplets in electrospraying [23]. The solution will become a conical droplet, a Taylor cone, when using a higher molecular weight polymer. Due to sufficient chain entanglement structure, hydrophobic interactions, and hydrogen bonds of the polymer lead to a stable, continuous fiber formation instead of droplets. When the electrostatic force overcomes the surface tension, it stretches the jet stream causing it to elongate as a filament. This filament solidifies and is eventually deposited on a grounded collector, these ultrafine fibers will form, and this process is then called electrospinning [24].

1.1.1. ELECTROSPINNING

Electrospinning is a technique that transforms polymer solutions into micro- or sub micro dimensioned fibers under the effect of a high-voltage electric field, making it as a versatile method for fabricating nanofiber materials comprised of various polymers and ceramics [25]. Electrospinning is known for its simplicity, flexibility, and multipurpose nature in fabricating submicron-scale fibers [26]. The basic setup of electrospinning comprises the key components of a high-voltage power supply, a needle spinneret, and a grounded collector, alongside key parameters contributing to the successful fabrication of nanofibers (Figure 1.1). Electrospinning utilizes either a melted polymer or a solution, but its viscosity and conductivity must be appropriate to ensure effectiveness during the process. The solution forms into a droplet due to surface tension at the needle tip. Surface tension was countered upon the application of a high voltage electric field which caused the droplet to turn into a cone shaped structure known as a Taylor cone. These forces when applied caused the surface tension to be completely overpowered producing a charged jet that was ejected towards the collector. The jet became very thin and long due to electrostatic forces causing it to be stretched as it travelling. There was the evaporation of solvent particles thus leading to the solidification of the polymer. Fibers that had solidified were then deposited into the opposite charged or grounded collector forming mesh or mat which

didn't have a weave pattern [27], [28]. Fiber morphology, structures and functions can be significantly influenced by the process, solution, and the environmental parameters [29].

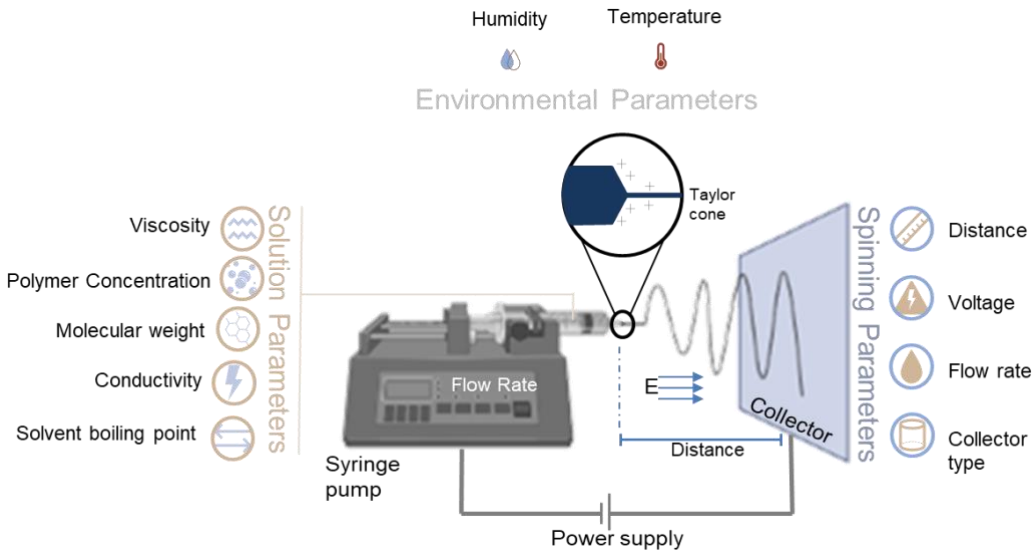

Figure 1.1: Scheme of electrospinning process and the parameters that affect the process [7].

One of the advantages of this method is its ability to combine a variety of natural and synthetic polymers, along with inorganic materials, to effectively produce micro/nanocomposite fibers with the multifunctionality that they bring. Moreover, the high-surface area, porosity, and the capability of loading drugs or other biomolecules into the fibers make them useful for different applications [30], [31].

In tissue engineering and biomedical applications, the fabrication of electrospun nanofibers using both synthetic and natural polymers have gained significant attention. The use of synthetic polymers in electrospinning is advantageous due to their mechanical stability, biocompatibility, biodegradability, and non-toxicity, making them suitable for biomedical applications. However, many synthetic polymers usually processed by electrospinning often require the use of chemically aggressive organic solvents, with relevant limitations in the manufacturing of cell-friendly substrates. Accordingly, the main constraints associated with the use of toxic solvents in electrospinning are paving the way to the use of less or non-toxic solvents (e.g., water, ionic liquids), so limiting the use to a

restricted group of green polymers with more sustainable properties (e.g., PVA, PEO). Alternatively, they are increasingly used in combination with natural polymers, such as proteins of polysaccharides with native function biological recognition [32], [33]. Additionally, by a large customization of the electrospinning setup (i.e., needles, collectors), it is possible to fabricate scaffolds with a controlled spatial distribution of fibers, in order to meet the structural organization of different tissue types (e.g., muscle, bone, skin, nerve) [8].

1.1.2. ELECTROSPRAYING

Electrospraying is an EFDT that involves the liquid atomization of a polymeric solution influenced by a high voltage, as in the case of the electrospinning technique. The electrospraying technique has been used for the fabrication of micro- or nanoparticles employed in several biomedical applications, particularly for drug delivery system (DDS) [34], [35], [36]. The main difference between both EFDTs is related to the polymer concentration (Figure 1.2). For electrospraying, low concentrations are preferred to allow the jet to break into small liquid droplets. The formed droplets are highly and identically charged, which prevents their agglomeration and allows their dispersion in the space [37].

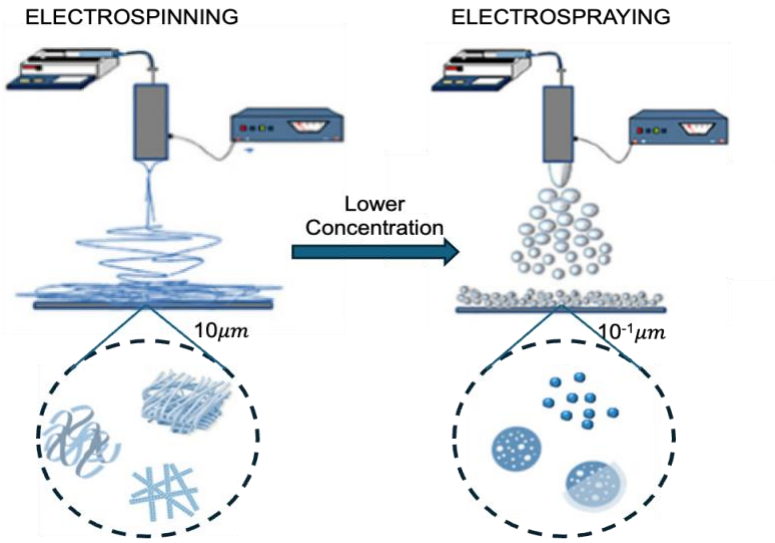

FIGURE 1.2: Schematic representation of the morphological properties of products via electrospinning and electrospraying techniques [7], [8].

The basic setup is similar to the electrospinning technology and consists of a high voltage power supply, a syringe with a metallic needle connected to a syringe pump and the grounded collector. During the electrospraying process, electrical forces overcome the surface tension of the droplet under the influence of an external electric field. Moreover, solvent evaporation allows the collection of solid particles. The size, morphology, and surface of particles can be modified and controlled by process parameters such as flow rate, applied voltage, and polymer concentration [38], [39]. For instance, different morphologies of particles, such as spheres, donut-like, and corrugated shapes with sizes ranging from several tens of microns to hundreds of nanometers, were observed to be influenced by polymer molecular weight and concentration, solution flow rate, voltage, and solvent [40]. In particular, micro- or nanoparticles via electrospraying have been fabricated for drug delivery applications, due to their high loading efficiency and narrow size distribution. Electrospraying is a one-step process, compatible with different biomaterials (e.g., natural and synthetic polymers) that can act as carriers of a wide variety of molecules and drugs (e.g., water or poorly water-soluble drugs) [41], [42]. Congruently with electrospinning, the use of organic solvents in electrospraying poses some limitations, as it can potentially

harm the bioactivity of biomolecules (i.e., proteins, genes, enzymes), also compromising the transmembrane interaction with cells. However, the electrospray is a process mainly driven by the solvent evaporation, so that the use of harmless or aqueous solvents impose to adopt further solutions, such as the use of additives or other compounds, to promote efficient interactions of polymer solution with electrical forces in the face of some effects in terms of particle size—only micrometric and shape not spherical/eccentric [43].

1.2. SETTING OF PARAMETERS

In the electrospinning process, many parameters determine spinnability and the final product's morphology and uniformity of nanofibers. Different nanofibers with different morphologies can be fabricated by sagely dosing and combining these parameters in uncountable ways. Solution-dependent parameters (i.e., viscosity, polymer concentration, solvent type, surface tension, electrical conductivity, and molecular weight) and environmental conditions, such as humidity and temperature, directly affect spinnability [7].

All these variables have a direct impact on the manufacture of smooth, bead-free electrospun fibers, therefore a thorough understanding of these parameters is essential to getting insight into the electrospinning process and the production of polymeric nanofibers. This is because the properties of nanofibers may govern their applications [44].

1.2.1. SOLUTION PARAMETERS

1.2.1.1. POLYMER CONCENTRATION AND VISCOSITY

The characteristics of the resulting nanofibers are greatly influenced by the molecular weight and viscosity as well as the polymer concentration during the electrospinning process. Higher molecular weight polymers enhance the viscosity of the spinning solution, which is crucial for fiber formation. Specifically, studies indicate that only solutions above a certain entanglement concentration yield uniform fibers, particularly with high-molecular-weight [45]. The concentration of the polymeric solution plays a critical role in determining the morphology of electrospun fibers by directly influencing the jet's

stretching behavior. Increasing polymer concentration generally leads to thicker fibers due to enhanced mass flow during the electrospinning process [46]. It was found that bead formation was reduced with increasing the polymer concentration and/or molecular weight. More particularly, studies indicate that low polymer concentration can hinder the entanglement necessary for stable fiber formation, causing the jet to break up into beads due to the chaotic oscillation of the charged jet [47]. Fiber diameter increased correspondingly to increasing concentrations for all molecular weights. Furthermore, increasing the concentration beyond a critical value (the concentration at which beadles uniform nanofibers are formed) hampers the flow of the solution through the needle tip (the polymer solution dries at the tip of the metallic needle and blocks it), which ultimately results in defective or beaded nanofibers [48]. When the chain entanglement in a polymer solution is inadequate as seen in the viscosity index, it results in the formation of droplet jets which are neutral with respect to the electric field due to their low surface tension value. This gives rise to what is known as the Rayleigh Instability, which is the tendency of the liquid jet to break up into several smaller droplets . This is caused by the forces acting on the fluid and the surface tension that is present in the fluid [44]. The morphologies of the beads depict an interesting shape change from a round droplet-like shape (with low-viscosity solutions) to a stretched droplet or ellipse to smooth fibers (with sufficient viscosity) as the solution viscosity changes [49].

1.2.1.2. Solution Conductivity

Increased solution conductivity promotes charge build up, leading to a more distinct formation of the Taylor cone and improved stability of the jet. This therefore reduces Rayleigh instabilities and improves the whipping which results in smaller and uniform fibers. Conversely, reduced conductivity can result in irregular jet formation and unstable Taylor cones, ultimately affecting the uniformity and consistency of nanofiber production. For instance, the conductivity of the polymer solution modifies the stretching / elongation of the jet as well as the size and morphology of the fibers. The conductivity of the solution can be increased by adding conductive additives like, for instance, salts or metal nanoparticles. Also, changes in solvent composition or use of solvent systems can change

the conductivity of a solution. However, the increase of conductivity has to be controlled, since it can interfere with the viscosity of the solution and the interactions with the solvent [44].

1.2.1.3. SOLVENT EFFECTS

Appropriate attention must be paid to solvent characteristics in order to get the best fiber formation, morphology and quality. Among these parameters, a desirable solvent is one that can adequately dissolve the polymer, has a moderate degree of volatility to allow for evaporation during the process, and also has flow and surface tension properties that allow for the formation and stretching of the jet. The compatibility of the solvent with the polymer also enhances the uniformity of the nanofibers and inhibits bead formation. In addition, the selection of solvents in electrospinning is critical due to several factors, including toxicity, environmental impact, and ease of removal post-processing. Toxic solvents, such as dimethylformamide (DMF), pose health risks and can lead to the release of volatile organic compounds (VOCs) during electrospinning, which adversely affects indoor air quality and cellular viability when used in biomedical applications [50]. Recent studies advocate for the use of benign solvents, like dimethyl sulfoxide (DMSO) and acetic acid, which mitigate these risks while still achieving desirable fiber properties [51]. Moreover, the environmental implications of solvent use necessitate a careful evaluation of solvent selection, as the choice can significantly influence the sustainability of the electrospinning process [52]. Thus, solvent selection must be approached as a multifaceted process, considering not only the immediate effects on fiber formation but also long-term environmental and health consequences [53].

The preferred solvents for electrospinning process have polymers that are completely soluble. Second, the solvent should have a moderate boiling point. Its boiling point gives an idea about the volatility of a solvent. Volatile solvents are generally preferred as their high evaporation rates encourage the easy evaporation of the solvent from the nanofibers during their flight from the needle tip to the collector. However, highly volatile solvents are mostly avoided because their low boiling points and high evaporation rates cause the

drying of the jet at the needle tip. This drying will block the needle tip, and hence will hinder the electrospinning process. Similarly, less volatile solvents are also avoided because their high boiling points prevent their drying during the nanofiber jet flight. The deposition of solvent-containing nanofibers on the collector will cause the formation of beaded nanofibers [49].

1.2.2. Process Parameters

1.2.2.1. Applied Voltage

The voltage that is applied is essential in electrospinning as it is the main force of making fibers. As mentioned before, the voltage that is applied causes the droplet of polymer solution at the needle tip to be stretched and deformed, hence causing the Taylor cone to form. Once the voltage reaches a critical threshold jet formation is triggered, and the jet proceeds along a linear trajectory [54]. The critical voltage varies among different polymer systems, and optimizing this value is essential to achieve optimal morphology in the resulting fibers. At large scales, it has been demonstrated that an applied voltage results in the amplification of repulsive forces which leads to reduction of fiber diameter owing to stretching [44].

This polymer solution stretching upon elongation of the electrospinning voltage reduces its diameter and result in reduced fiber diameter in the nanofibers. An increase in the applied voltage beyond the critical value will result in the formation of beads or beaded nanofibers. The increases in the diameter and formation of beads or beaded nanofibers with an increase in the applied voltage are attributed to the decrease in the size of the Taylor cone and increase in the jet velocity for the same flow rate [49].

1.2.2.2. Flow Rate

The flow rate, also referred to as the feed rate, is defined as the velocity at which the polymer solution is delivered to the needle, ensuring a consistent supply of the charged jet. The interaction of the feed rate with the spinneret diameter and applied voltage

determines the rate of polymer solution ejection from the spinneret. In order to maintain a constant Taylor cone and have enough time for the solvent to evaporate, controlling the flow rate is very important. Otherwise, the morphology of the nanofibers obtained may be affected, for example fiber diameter, beading and uniformity. Flow rates below the critical threshold lead to the development of an asymmetrical Taylor cone, consequently resulting in broader distributions of fiber diameter, charged jet instability, marked by frequent receding and reformation of the Taylor cone [55]. This instability leads to intermittent flow and strand breakages. Higher flow rate result in a multi-jet pattern, which correlates with larger bead diameters and an increase in defects and ribbon-like structures due to incomplete drying of the porous fibers [56]. The formation of beads and with an increased flow rate was mainly attributed to the non-evaporation of the solvent and low stretching of the solution in the flight between the needle and metallic collector [49]. Minimum flow rate is preferred to maintain a balance between the leaving polymeric solution and replacement of that solution with a new one during jet formation. This will also allow the formation of a stable jet cone. In electrospinning, the average flow rate can vary greatly as a function of the polymer solution however this characteristic takes different values according to the literature. Thus, it is necessary to optimize the flow rate in order to establish the best working environment for the particular electrospinning process experimentally [44].

1.2.2.3. NEEDLE TO COLLECTOR DISTANCE

The distance from the needle to the collector in electrospinning, which is also called working distance provides a route for the charged polymer jet as it travels. Like many other parameters, the needle-to-collector distance also has a range of limits for different polymer systems. As a rule, when the working distance is less, travel time is also short, hence the time for solvent evaporation is also short. On the other hand, increasing the distance between the needle and the collector increases the time taken for the jet to stretch which means longer and thinner fibers would be formed [57]. But over doing this, past a reasonable threshold, it is likely to decrease the strength of the electric field which of course raises Rayleigh instability. Such a situation will cause the fiber diameter to widen and

become less uniform with many defects [58]. For these reasons, it is important to strike a balance and set the optimal working distance enabling evaporation while able to maintain the potential developed [44].

1.2.2.4. NEEDLE DIAMETER

Dimensional parameters of the needle in electrospinning determine the volumetric flow rate of the polymer solution as well as the degree of stretching of the ejected jet. An increase in the needle opening diameter serves to increase the flow of the polymer solution, so that thicker fibers can be obtained due to insufficient stretching. On the other hand, a smaller needle diameter enables flow rate to be lower allowing for greater stretching of the jet hence finer fibers can be obtained [59].

1.2.3. AMBIENT PARAMETERS

Humidity cause changes in the nanofibers diameter by controlling the solidification process of the charged jet. Temperature causes two opposing effects to change the average diameter of the nanofibers: (i) it increases the rate of evaporation of solvent and (ii) it decreases the viscosity of the solution. On the one hand, an increase in the evaporation of the solvent and decrease in the viscosity of the solution work by two closely related mechanisms, both lead to decrease in the mean fiber diameter [49].

1.3. APPLICATIONS OF EFDTS IN BIOMEDICAL FIELD

1.3.1. TISSUE ENGINEERING

The emergence of EFDTs is revolutionizing biomedical applications due to the versatility that these techniques offer, particularly in the fabrication of micro and nano structures of specific dimensions, shapes, and functional capabilities. The many uses of these techniques cut across different spheres, thus showcasing versatility and the potential for advancement in healthcare.

Production of 3D porous scaffolds comprising of large amounts of fibrous structure with high porosity and a large surface area can be achieved through electrospinning. Fabricating

porous 3D fibrous scaffolds that mimic the natural properties of the extracellular matrix (ECM) makes electrospun fibers attractive for tissue engineering. Whenever scaffolds are designed for tissue engineering, it is imperative that they allow for cell attachment, proliferation, and further differentiation in tissues. A key feature of a material to be used in tissue engineering is its ability to be integrated with the tissue. It should possess the ability to degrade over time in a non-destructive manner. Moreover, factors such as the degree of fiber orientation and porosity provided in the design do enhance the subsequent integration. For instance, aligned fibers tend to dictate the organization and functionality of cells populated in the engineered neural tissue. Indeed, astrocytes and other glia are more aligned and change in shape more readily when placed on aligned nanofibers, thus aiding the neural repair and regeneration process [43].

1.3.2. Drug Delivery

The pharmaceutical field has experienced a rise in the development of new promising and innovative drug delivery approaches including the field of nanotechnology such as nanoparticles and nanofibers [60]. Nanofibers made from biodegradable and biocompatible polymers have gained interest due to their exceptional versatility, effectiveness, and distinctive physicochemical properties such as significant surface area, small diameter, and high aspect ratio. EFDTs further develop fabrication involving drug delivery applications using nanofibers and drug delivery microparticles. Nanofibers optimize the delivery of the drug through their rigid structure that has the ability to contain and safeguard active ingredients [61]. On the other hand, electrospraying technology produces a wide range of uniform microparticles which are effective in targeting specific receptors thus improving the efficacy of treatment by avoiding relevant side effects [62]. Engineering of the drug release profiles can be achieved through the modification of the polymer composition, solvent systems, and drug containing fiber/microgel structure.

1.3.3. Wound Healing

These scaffolds mimic the ECM, promoting cell adhesion and proliferation, which is crucial for wound healing [63]. The incorporation of bioactive molecules, such as antibiotics and

growth factors, into these scaffolds significantly enhances their functionality. For instance, scaffolds loaded with mupirocin and keratin have demonstrated antibacterial properties, reducing infection risks. Additionally, scaffolds designed for sustained drug release can improve tissue regeneration by delivering therapeutic agents directly to the wound site, thereby enhancing tissue development and minimizing systemic side effects [64]. The versatility of electrospun materials allows for the customization of scaffold properties, optimizing them for specific therapeutic applications [65].

1.3.4. Bioelectronics and Sensors

EFDTs can also be used for bioelectronics where sensors and other implant covers possess conductive fibers in them. For instance, nanofibers containing conductive fillers like MXene or graphene enhanced electrical properties and thus can be used for biosensors and neural interfaces [66], [67], [68].

1.3.5. Biofiltration

The nanofibrous membranes that are manufactured via EFDTs method are applicable in biofiltration and hemodialysis due to their cause high porosity and selective mass transfer. This allows for effective removal of contaminants from biological fluids, blood purifying and even water treatment [69], [70].

1.4. Conclusion

EFDTs have exhibited incredible possibilities in fabrication micro and nanoscale materials in a versatile and cost effective manner. This chapter has described the concepts, processing parameters and areas of use of EFDTs, stressing their capability of adoption for various biomedical and environmental uses. The EFDTs have however been successful in targeting the biomedical industry though scalability, biocompatibility as well as getting the legal approval is still an issue. The use of certain organic solvents in some EFDT processes creates concerns about on the residual toxicity and environmental pollution. Research is underway to formulate more environmentally friendly solutions like water based

electrospinning to deal with these concerns. The prospects of EFDTs in the field of medicine is thanks to the enhancement of materials science, better process techniques and combination of many fields towards the production of new generation tools for therapy and diagnostics.

Chapter 2

2. MULTICOMPONENT POLYMERIC PLATFORMS FOR BIOMEDICAL APPLICATIONS

In the manufacturing of nanofibers, which involve the use of various polymer blends and different operational conditions, electrospinning is widely used. However, it is important to choose the right polymers for the task, especially when it comes to medicinal preparations because they must be bio-degradable, bio-compatible, and biologically hydrophilic. This is because hydrophobic polymers create a gradual release profile for the drug, as they limit the binding angle with aqueous solutions. In contrast, hydrophilic polymers are beneficial when fast release of drugs is required, as they facilitate release by swelling and dissolution. Moreover, even the crystallinity of the polymer affects the release of the drug, remembering that the amorphous region promotes interaction with water thereby quickening the release.

2.1. MATERIALS USED IN EFD TECHNIQUES

The efficiency of using the process for any useful tissue engineering application will be further decided by bioactive groups incorporated into artificial ECM structures [43].

2.1.1. NATURAL POLYMERS

Natural polymers are extracted from various sources, including plants and animals. These include cellulose, starch, chitosan, and silk. With the advancement of biotechnology, polysaccharides, proteins and biopolymer derivatives constituting each natural polymer category are widely employed in drug delivery systems owing to their good features such as biocompatibility, biodegradability, low toxicity, ready availability and even possible

inherent antibacterial activity and even greater therapeutic usefulness like collagen and hyaluronic acid [71]. Natural polymer-based nanofibrous scaffolds hold significant promise for diverse skin tissue applications, encompassing wound dressings and controlled drug delivery. Their structural is similar to the extracellular matrix with high water retention capacity which make them excellent candidates for therapeutic interventions [44].

The electrospinning method has been utilized to generate non-woven mats for tissue engineering using different natural biopolymers including proteins (gelatin, collagen and silk fibrinogen) and polysaccharides (chitosan, hyaluronic acid and cellulose). These natural polymers provide many of the instructive cues required by the cells attachment and proliferation and on the other side have the problem of batch-to-batch property variation [72].

There is a growing use of natural polymers in EFDTs such as electrospinning and electrospraying for the production of nanofibers and nanoparticles for biomedical applications. For example, gelatin and collagen can be utilized to replicate the architecture and at the same time the function of the extracellular matrix optimizing the microenvironment for the cells and their functions. Chitosan and hyaluronic acid also possess excellent biocompatibility and antimicrobial properties thus they are frequently used in the manufacture of scaffolds for wound healing and drug delivery systems. On the other hand, the hydrophilic tendencies of these polymers can compromise the structural integrity of the nanostructures thereby limiting their use, which makes necessary post-treatment or blending with synthetic polymers.

2.1.2 Synthetic Polymers

Exciting advances in these fields have resulted in the invention of materials that naturally combine with the human body, such as synthetic polymers. Chemical processes allow for the manufacture of synthetic polymers, which in turn permits human control over reproducibility in a multitude of factors such as mechanical strength, thermal resistance and decomposition rate. One aspect at which synthetic polymers surpass natural ones is

their true reproducibility, resulting from the ability to redefine their chemical composition and hence altering what is expected. Among those used are polylactic acid (PLA), polycaprolactone (PCL), and poly(vinyl alcohol) (PVA) [9], [73], [74].

To design scaffolds with optimal mechanical and biological characteristics, tissue engineering often utilizes synthetic polymers alone or in combination with natural polymers. Moreover, these materials have been electrospun, electro-sprayed, and 3D printed to suit applications like tissue regeneration, drug delivery, and wound healing. The issue, however, is that unlike natural polymers, synthetic polymers tend to not have bioactive cues which can diminish their biocompatibility. In order to fix this issue, synthetic polymers are often functionalized or mixed with other bioactive substances [75], [76].

PVA is one of the most commonly used synthetic polymers in biomedical applications, particularly in EFDTs. It consists of $[CH_2CH(OH)]_n$ repeating units. This polymer composed of vinyl monomers is not prepared directly from vinyl alcohol because of its instability, which induces a tautomerization mechanism to acetaldehyde [77]. PVA is a synthetic and semicrystalline polymer with multi-hydroxyl groups, with an excellent oxygen barrier, dyeing properties, and mechanical strength. The physicochemical properties of PVA are closely related to its preparation method and, in particular, to the state of hydrolysis, which can be either complete or partial. The synthesis conditions allow for different molar masses, solubility, and adhesion or mechanical characteristics. These two parameters are known to have a significant influence on the processability and performance of this polymer. Thus, as the degree of hydrolysis increases, so do the crystallinity, melting temperature, and mechanical strength due to the high level of hydrogen bonding between the chains. It has good mechanical performance, high tensile strength and flexibility, and oxygen and aroma barrier properties. In addition, it is odorless and non-toxic and has excellent film-forming, emulsifying, and adhesive properties. However, as a water-soluble polymer, water molecules act as a plasticizer, decreasing tensile strength while increasing its elongation at break. It is a semi-crystalline and biodegradable polyhydroxy polymer and has been studied intensively due to its good

thermal stability, biocompatibility, chemical resistance, hydrophilicity, biocompatibility, and biodegradability, and inexpensiveness [9], [78].

PVA is hydrophilic in nature and thus helps to form homogenous fibers or particles in EFDTs. The mechanical characteristics and the handling of PVA can be improved by blending the polymer with natural polymers like gelatin or chitosan and creating nanostructures that replicate the extracellular matrix's structure [79]. Besides, PVA has a great advantage in drug delivery systems and wound healing as it can serve as a carrier for bioactive drugs. On the contrary, its water solubility and high moisture sensitivity may require remedial processing treatments or chemical crosslinking to improve stability [80].

2.1.3. Combination of Natural and Synthetic Polymers

Synthetic polymers offer superior mechanical strength, processability, and stability, but they are lacking in bioactivity, which restricts their applications in tissue engineering. On the other hand, natural based polymers are active and help with cell attachment, proliferation, and differentiation but their structure and mechanical properties are not always strong enough for some advanced biomedical applications.

In order to tackle these issues, the incorporation of natural and synthetic polymers has proven to be an effective technique in the development of EFDTs. With this synergistic combination, it is possible to fabricate scaffolds with natural polymers that are active and biocompatible while synthetic ones have sought strength, stability and customizable degradation rates. For instance, blending PVA with gelatin or chitosan not only improves the bioactivity of the resulting scaffold but also ensures better processability and stability [81], [82].

As components with two materials are successfully used in controlled drug delivery, wound dressings, and tissue engineering scaffolds, more advanced performance is obtained in comparison to a single component system. The two classes of materials integrated into a single system emphasize the need for cross discipline who's who for the design and development of next generation biomaterials for specialized biomedical applications.

2.2. Definition and Classification of Multicomponent Polymers

Especially in recent years, interest in polymers obtained from renewable resources has increased; thus, natural polymers, synthetic polymers from natural monomers, and polymers from microbial fermentation are frequently investigated. Similar to other petroleum-based polymers, polymers from renewable resources are rarely used alone, and many of their properties can be enhanced through blending and composite formation [7], [83].

2.2.1. Polymeric Blends

Polymer blend is a single-phase substance obtained by mixing two or more polymers, generally without strong chemical bonds. Researchers can produce materials with specialized and synergistic qualities by manufacturing nanofibers with multiple components, which makes them ideal for a wide range of applications. In the realm of tissue engineering, fibers hold great significance and composite electrospun fibers can be used in a variety of biomedical applications, such as the engineering of neural tissue. Research has shown that neural cells have the ability to find and use the cues provided by the fibers for migratory purposes while incorporating them into hybrid matrices, suggesting the possibility of using custom-fabricated fibers to influence cellular constructs [84].

The specific components used rely on several variables, including mechanical qualities, biocompatibility, chemical properties, conductivity, and the intended use of the neural tissue engineering scaffold [85]. By altering the mechanical properties of the final product, blend materials can be created to incorporate a variety of capabilities for uses like controlled drug delivery. It is possible to introduce extra characteristics like conductivity to affect biological activity by modifying fiber chemical features. Moreover, other components enable the delivery of topographic signals to central nervous system (CNS) cells, hence broadening the scope of possible uses. Moreover, multicomponent integration

can improve the overall stability and strength of nanofibers and by applying it with different collector assemblies, alignment as well as fiber morphology can be controlled [8].

Every component of a composite nanofiber can be functionalized in blend systems to fulfill a particular role. For instance, one component may provide structural support, and another may contain bioactive chemicals, thereby granting the material-controlled release capability. Multiple capabilities may be included into a single nanofiber system thanks to this functionalization.

2.2.2. COMPOSITES

Polymeric composites are multi-phase composite systems made from a polymeric and/or non-polymeric material or a combination thereof for the purpose of improving their inherent properties through physical or chemical bonding. As a result, these systems are particularly useful for biomedical applications since they are able to integrate different material properties into one system/panel [86].

Such enhancing elements target certain properties like mechanical strength, thermal resistance, or electrical conductivity. Carbon nanotubes (CNTs), graphene oxide (GO), hydroxyapatite (HA), and various metallic or oxide nanoparticles are some of their representatives. Depending on the application, these reinforcements can confer bioactivity, differentiation or enhance electric conductivity [87], [88], [89], [90].

2.3. MECHANICAL AND CHEMICAL PROPERTIES OF POLYMERIC COMPOSITES AND BLENDS

The performance of polymeric composites and blends can be influenced by their mechanical properties such as tensile strength, elasticity and toughness. These properties can be achieved by integrating polymers with reinforcing agents or through the synthesis of natural and synthetic materials. For example, natural polymers like gelatin, chitosan or silk fibroin are bioactive and compatible with biological systems while synthetic polymers like PVA and PCL enhance mechanical properties and reduce degradation rates. This

combination improves the material's performance in mimicking tissue engineering extracellular matrices [91], [92]. Furthermore, the chemical properties of blends such as solubility, stability, and resistance to environmental effects can also be enhanced by blending. For instance, moisture absorption and the durability of composites can be improved by incorporating hydrophobic materials with hydrophilic ones [74].

As applied in EFDTs, these advancements are of great significance. According to recent studies, the use of natural and synthetic polymers simultaneously aids in the manufacturing of either defect free nanofibers or particles who have the desired mechanical and biological properties. Not only does blending assist in improving the spinnability and uniformity of the solution during electrospinning but it also increases the drug delivery system's efficiency and cell-biomaterial interaction [93], [94]. These hybrids clearly illustrate how the combination of natural and synthetic polymers can help in elimination of the shortcomings of individual materials so as to fabricate scaffolds and materials suitable for biomedical purposes.

Finally, the combination of natural and synthetic polymers in composites facilitates the fabrication of structures which have bioactive properties of natural polymers and synthetic polymers, the strength and processability [9]. This strategy emphasizes the meaning of materials design for improvement of the wide range of applications from tissue engineering to drug delivery.

2.4. CONCLUSION AND FUTURE REMARKS

Multicomponent polymeric systems have established themselves as enabling technologies in biomedical applications in the areas of tissue engineering, drug delivery, wound healing and other. It is worth to mention that the development of such materials involves blending natural and synthetic polymers, whereby the bioactivity of natural constituents is coupled with mechanical strength and tunable properties of synthetic polymers. The use of EFDTs, in this respect, has increased their potential by enabling the fabrication of customized multi-functional scaffolds.

Nonetheless, concerns like the need for effective dispersion of fillers, consistency in production and the scarcity of source materials in natural polymers still remain major challenges. Research efforts should direct the use of environmentally friendly production techniques such as electrospinning in solvents such as water, and new bioactive fillers that will increase biological performance. The ability to modify the design of the scaffolds by using advanced manufacturing technologies such as 3D bioprinting also opens new avenues for patient-specific applications.

These challenges will require closer interdisciplinary cooperation in order to allow the clinical development of these materials. As long as progress in the design of new materials or improvement in their processing approaches continues, it can be expected that multicomponent polymeric systems will become major constructs in the biomedical field.

Chapter 3

3. PREPARATION AND OPTIMIZATION OF PVA BASED NANOFIBERS

PVA is one of the most attractive polymers with a wide range of uses because of its water solubility, biocompatibility, low toxicity, good mechanical properties, and relatively low cost [78]. Different molecular weights—from 20,000 to 400,000 g/mol—and hydrolysis degrees—ranging from 86 to 98%—concur to significantly influence its physical/chemical properties (i.e., mechanical properties, melting point, light transparency) and sensitivity to external stimuli (i.e., pH, temperature) [95], [96]. PVA is water-soluble, slightly soluble in ethyl alcohol, and insoluble in other organic solvents. Its main benefit is that PVA preferentially dissolves in water near the boiling point, thus making it challenging to form stable substrates at room and body temperatures. Moreover, its highly tunable viscoelastic properties make PVA suitable for a large variety of manufacturing processes for fabricating devices in different forms, such as hydrogels, sponges, films, membranes, and fiber [97]. It can be easily combined with other polymers or additives to form multicomponent systems (i.e., blends, composites, hybrids) with improved functions to support cell interactions and related biological events [98] [99].

The electrospinning of the PVA solution has been extensively studied for the preparation of ultrafine separation filters, biodegradable mats and inorganic fibers. the ionotropic behavior of PVA well supports interaction with high-voltage electric fields, promoting the fabrication of sub-micrometric fibers with peculiar topographic signals which play a relevant role in influencing in vitro interactions with cells [100]. In the last decade, PVA has been extensively studied to prepare micro-/submicron-structured membranes via electrospinning for different applications [101]. Although there is a high reproducibility of

the electrospinning process that can be variously adapted to a wide range of polymers and polymeric solutions, increasing attention is being devoted to the fabrication of PVA nanofibers for tissue engineering applications, owing to some of its superior properties, such as good fiber-forming ability, thermal stability, good mechanical properties, and low cost [102], [103]. Moreover, the preparation of PVA electrospun fibers does not require the use of aggressive organic solvents, drastically limiting the risks associated with toxicity and carcinogenicity, but only aqueous solutions currently offer the most green and sustainable pathway for biomedical applications [104], [105].

However, inert bioactivity, poor stability and fibers in this form tend to be rapidly dissolved in any aqueous solution due to the high surface-to-volume ratio of PVA which can compromise the efficiency of electrospun membranes for in vitro use. In this case, the molecular release and in vitro stability of the membranes can be also modulated by different chemical or physical strategies involving different functional groups (i.e., –OH) along its backbone chain to generate inter-chain links to improve its water stability and structural integrity [106]. Also, they can be combined with other polymers to increase the solution's spinnability. The assembly of multicomponent systems (i.e., blends, composites, hybrids) also offers the opportunity to cover the lack of individual component properties through the benefit of synergistic interactions among them which allow for improvement in their average specific properties and functions [107]. In this view, different approaches based on the blending with other polymers or additives, chemical backbones (i.e., copolymer compositions), or surface (i.e., grafting) modifications can be used to modify a wide range of polymer features [108], [109]

Herein, polyethylene oxide (PEO)—a water-soluble polymer with eco-friendly and benign properties [110], [111]—was proposed as a surfactant to stabilize fiber morphology. Moreover, gelatin—a protein obtained by the hydrolysis of native collagen fibers [112]—was offered as a bioactive agent to improve biocompatibility, promote cell interaction, and mimic the composition of fibrous components of the ECM. Previous studies have demonstrated that structural proteins, like gelatin alone, exhibit poor workability to form electrospun nanofibers due to strong hydrogen bonding. At the same time, when in

combination with other biopolymers, they can efficiently work firstly, by minimizing the jet instability phenomena able to promote the formation of beads along the fibers, and secondly, by improving polymer chain packing, with effects on the ultimate chemical and mechanical stability of the fibers [113], [114].

3.1. Materials and Methods

PVA (Mw 130,000 Da, 99+% hydrolyzed), PEO (Mv 300,000 Da), citric acid (ACS reagent, ≥99.5%) were all purchased from Sigma-Aldrich (St. Louis, MO, USA).

3.1.1. PVA Solution Preparation

Different PVA solutions with different concentrations—i.e., 8, 10 or 12% (w/v)—were prepared to optimize the electrospinning process. The PVA solution was heated to about 80°C and stirred (120 rpm) for 3 h. PEO (1% w/w with respect to the PVA) was added to the polymer solution, and the mixture was stirred (120 rpm) for 1 h at room temperature. Citric acid was added (10% w/w) to the solution 30 min before electrospinning as a green crosslinking agent.

3.1.2. Process Optimization and Post Processing

5 mL plastic syringe with a 27G metallic needle was connected to a high-voltage power supply, used as the source of the electric field, into a grounded chamber containing an aluminum foil covered collector (NANON01; MECC, Fukuoka, Japan)(Figure 3.1). It was placed into an additive syringe pump (KD Scientific, Holliston, MA, USA), vertically arranged with respect to the collector, to allow a controlled solution feed. An optimal set of process parameters was established in terms of voltage, flow rate, and electrode gap. The distance between the needle tip and the target was held constant at 25 cm. The difference in voltage between the needle and target varied from 19 kV to 21 kV. The flow rate of the polymer solution supplied to the syringe was fixed at 0.3 mL/h. All solutions were electrospun at room temperature under identical conditions for around 4 h, and relative humidity was kept at around 25%.

After the nanofiber production, samples were treated in the oven at different temperatures (90°C, 110°C, 130°C) for 15 min.

FIGURE 3.1: The electrospinning device used during the thesis work. This vertically aligned system facilitates the production of nanofiber matrices by transforming polymer solutions into fine fibers under high voltage.

3.1.3. CHARACTERIZATION

3.1.3.1. MORPHOLOGY

Optical microscopy (Leica DM750) and field-emission scanning electron microscope (Quanta FEG 200 FEI; Eindhoven, The Netherlands) with an accelerating voltage of 10 kV was used to evaluate the electrospun fibers' morphological features. Small pieces of rounded membranes were placed into the sputtering machine and coated with a Pd–Au

nanolayer to improve surface electroconductivity. Open-source image analysis software was used to measure average fiber diameters on selected SEM images (ImageJ 1.8; Fiji).

3.1.3.2. PHYSICAL AND CHEMICAL CHARACTERIZATION

Differential scanning calorimetry (DSC) (Q2000; TA Instruments) was conducted on PVA samples by single scanning and heating to 250°C at 10°C/min. Meanwhile, isothermal analyses at different temperatures (i.e., 90°C, 110°C, and 130°C) were performed on PVA samples to investigate the optimal conditions for fiber crosslinking. Thermogravimetric analysis (TGA) (Q500; TA Instruments) was carried out under an airflow, within a temperature range from 25 to 600°C and at a 10°C/min scanning rate. Fourier-transform infrared spectroscopy (ATR-FTIR Spectrum; PerkinElmer; Waltham, MA, USA) was performed from 650 to 4000 cm^{-1}.

3.2. RESULTS AND DISCUSSION

In the first stage, polymer concentration and molecular weight were properly selected in order to control the breakdown of the viscoelastic jet during the electrospinning process with effects on the final fiber structure. In particular, a morphological transition from beads to beaded fibers at lower concentrations (until to 8% w/v) was observed, then fibers were obtained as the PVA concentration increased (10–12% w/v), due to the progressive increase in the molecular entanglement concentration [115]. Morphological analyses via SEM were conducted in the case of fibers from a higher solution concentration (Figure 3.2). The PVA nanofibers showed an increase of their fiber diameter from 0.883±0.17 μm (10% w/v) to 1320 ± 0.24 μm (12% w/v), ascribable to the increase in viscosity and surface tension of the polymer solution. After 10% concentration selected, different electrospinning parameters also evaluated.

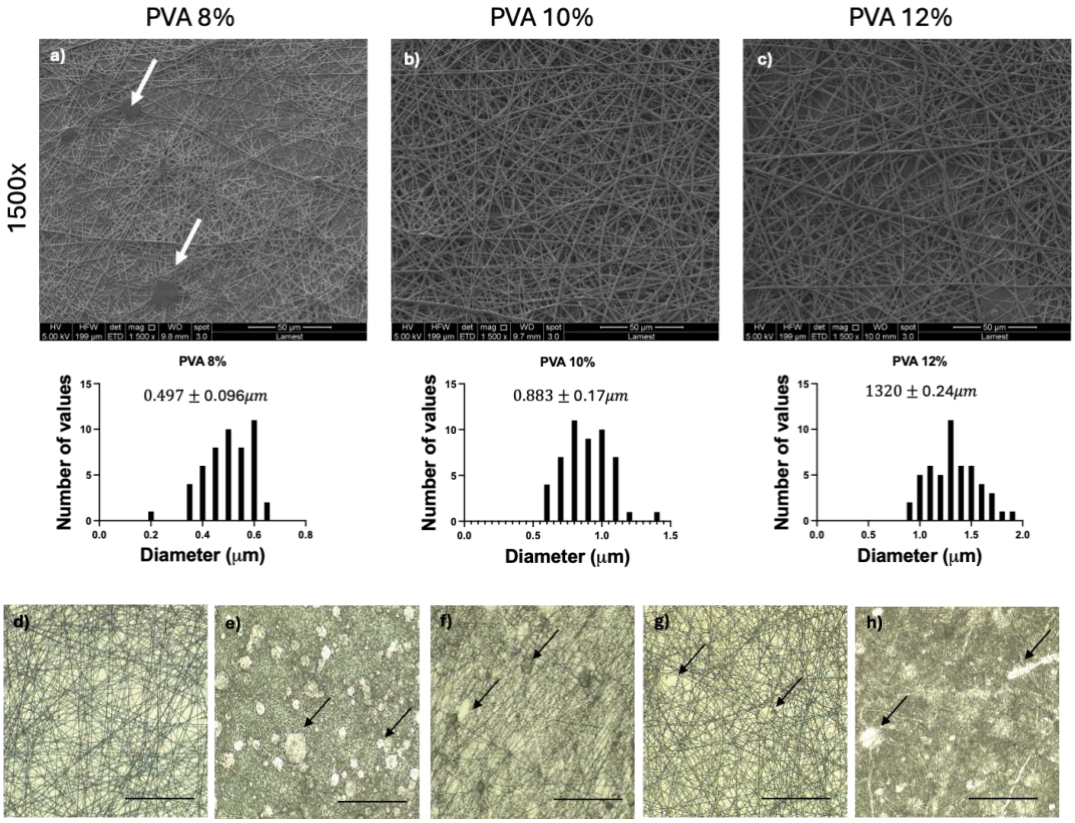

FIGURE 3.2: SEM images of electrospun fibers from different concentration solutions of PVA a) PVA at 8% presented beaded fiber, while fibers with 10% PVA b) a beadless fibres were obtained from and c) 12% (1500x magnification, scale bar: 50 µm). Comparison of optical images of electrospun PVA fibers produced with different electrospinning parameters d) optimal parameters (0,3ml/h, 20kv, 25cm), e) different flow rate (0.1ml/h, 20kv, 25cm), f) different voltage (0,3 ml/h, 18kv, 25 cm), g) (0,3 ml/h, 22kv, 25 cm) and h) different distance (0,3ml/h, 20kv, 15cm) (scale bar: 50µm) arrows show the defects.

TGA and DSC analyses (Figure 3.3) were also performed to investigate the physical and chemical properties of the PVA fibers. TGA highlighted a weight loss along an extended temperature range—from 230 to 420°C—which can be ascribable to the high polydispersion of molecular chains of used PVA. Moreover, the derivative graph shows three maximum points around 80°C, 261°C, and 419°C that indicate mass loss rates

associated with three distinct processes: adsorbed water loss, –OH functionalities, and pyrolysis [116]. Accordingly, the DSC analysis showed a melting temperature of PVA around 220°C in agreement with the literature [117].

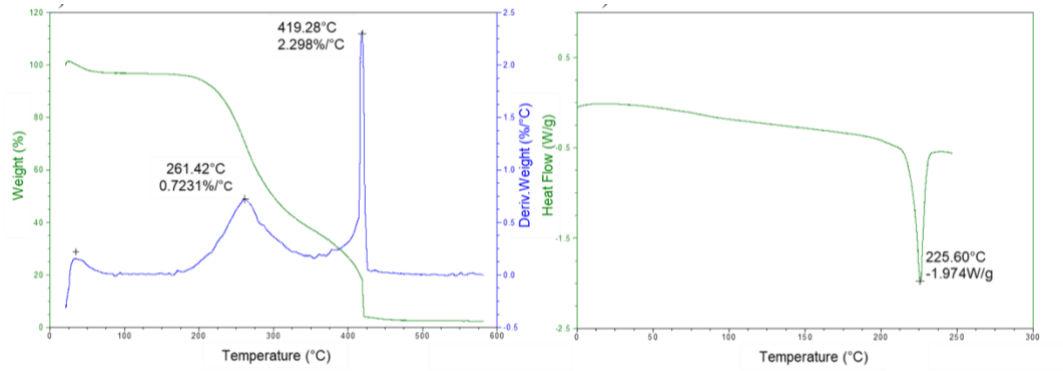

FIGURE 3.3: PVA electrospun fibers: comparative investigation of physical/chemical properties via TGA (left) and DSC (right) analyses.

In order to remove some defects caused by co-spraying/dropping phenomena during the electrospinning, small amounts of PEO were added to the polymer solution in order to stabilize the polymer jet during the formation of fibers, in accordance with previous experimental evidence [118], [119]. It was verified that PEO plays the role of a viscosifier agent, improving the spinnability of PVA solution without the use of further surfactants [120] and minimizing the formation of droplets along the fibers, not inducing unexpected problems in terms of cytotoxicity [121]. Previous studies have confirmed the good affinity of PEO with PVA in solution due to its water solubility at high concentrations and the ability of its long chains to form physical entanglement [122]. For instance, PEO was mixed into alginate solutions to improve the mechanical strength and stiffness of sodium alginate fibers [123]. This is due to the formation of additional hydrogen bonds between the hydroxyl groups and water molecules that reduce repulsive forces deputed to the formation of defects along the fibers.

In this work, it was proposed to use less than 3% of PEO to reach the right compromise between process stability and the morphological properties of fibers. Indeed, PVA is a polymer soluble in water, and electrospun fibers need to be crosslinked. In this view, a

green crosslinking method based on the use of citric acid was optimized. Citric acid is known as a non-toxic and inexpensive compound that was usually used to trigger the crosslinking reaction at elevated temperature—i.e., 120–190°C so that, it can be used only for a restricted number of biopolymers with appropriate melting point [124].

In order to optimize the crosslinking reaction, DSC analyses were performed by the isothermal route to evaluate the variation in heat flow versus time of membranes at different temperatures (90, 110, 130°C). Figure 3.4 shows a comparison of the crosslinking kinetic curves that indicate different thermal behaviors, mainly ascribable to the different exothermic heat released during the thermal reaction. At 130°C, a higher reaction was detected as remarked by the curve plateau. It was reached after 15 min, which is considered the required time to complete the crosslinking treatment. Fiber morphology was not affected after the crosslinking treatment, as confirmed by optical image analysis (Figure 3.4 b-d). Moreover, once immersed in water, non-crosslinked fibers completely dissolved, while crosslinked fibers maintained their shape, thus confirming the ability of crosslinking treatment to improve the stability of fibers. Additionally, it was recently reported that the use of CA—in place other toxic crosslinkers—improves the mechanical properties of fibers, compared to uncrosslinked ones [125], thus influencing their biological interface.

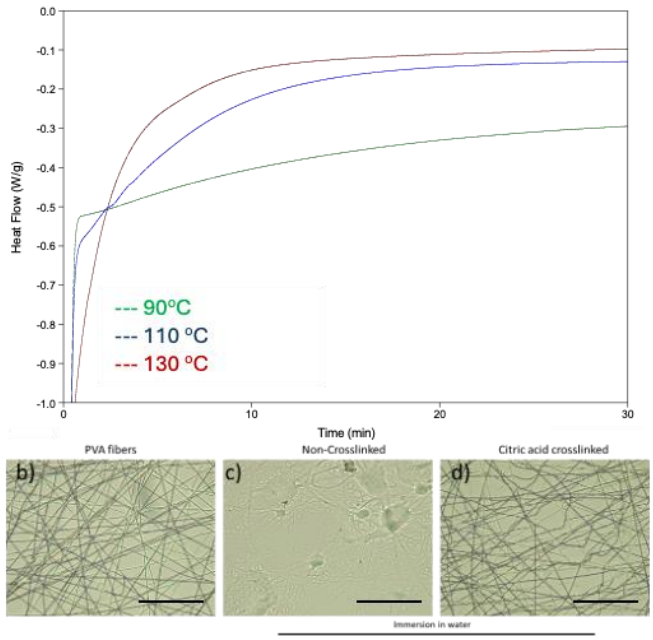

FIGURE 3.4: Thermal crosslinking of PVA/PEO nanofibers: a) isothermal analysis at 90°c (green), 110°c (blue), 130°c (red) and optical images of PVA non-crosslinked fibers b) before and c) after immersion in water and d) PVA crosslinked fibers after immersion in water.

Figure 3.5 summarizes the morphological studies—qualitative (i.e., SEM analysis) and quantitative (i.e., image analysis)—performed on crosslinked PVA (–PEO) and PVA/PEO (+PEO) nanofibers. It was possible to observe beadles fibers without relevant defects, with a decrease in the diameter of the fibers with PEO, mainly ascribable to the effect of the high molecular weight of PEO, able to improve the packing of PVA chains, with effects in terms of mobility and chain stretching [126], [127]. Moreover, it was verified that after thermal crosslinking, PEO is prone to volatize over 100°C which influences the diameter reduction in fibers [128], in agreement with the image analysis results.

FTIR analysis was also conducted to obtain further indications regarding the chemical composition of the fibers and interactions among the different phases (Figure 3.5 b). A broad peak around 3550–3200 cm^{-1} is attributable to the OH stretching vibration from the hydrogen bonds; 2980 and 2800 cm^{-1} refer to the stretching C–H group. After crosslinking with citric acid (+CL), a higher intensity absorption from 1710 cm^{-1} due to the C=O

stretching from aliphatic ester groups was detected. This is due to the chemical interaction between hydroxyl groups of PVA and carboxyl groups of citric acid [129].

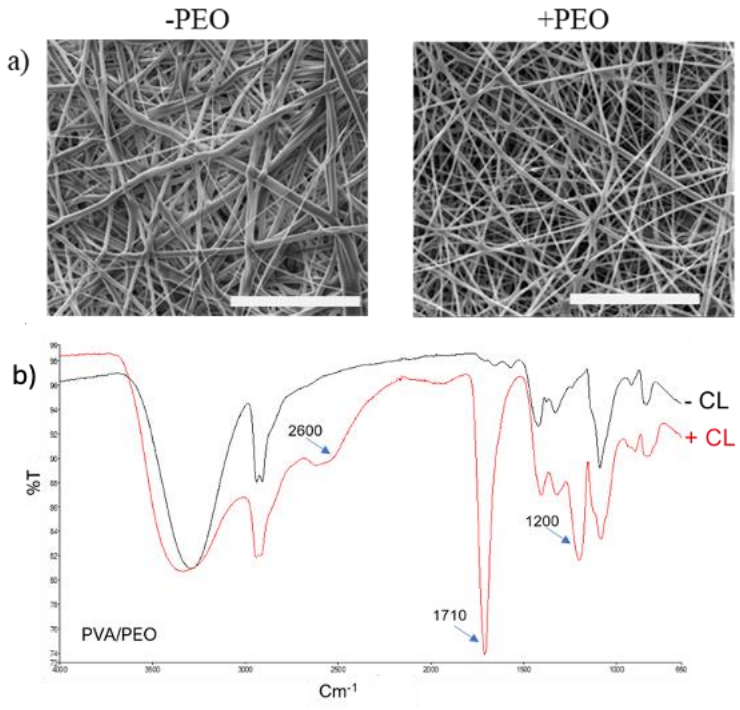

FIGURE 3.5: Crosslinked PVA(-PEO) and PVA/PEO (+PEO) electrospun fibers: a) SEM images (3000X magnification, scale bar: 40 µm) and b) FTIR analysis of samples with (red, +CL) or without (black, -CL) crosslinking.

3.3. Conclusion and Future Remarks

This research shows the potential of PVA as a suitable base material for electrospun nanofibers intended for biomedical purposes. The addition of PEO as a blending agent decreased the fiber diameter and imperfections, thereby improving the quality of the nanostructures better. These results point out that PVA/PEO based nanofibers can be used for tissue engineering applications with better structural properties suitable for scaffolding. In conclusion, the research underlines the significance of multi-component approaches in improving the mechanical, morphological, and functional characteristics of

electrospun fibers. The results create the opportunities for the development of future studies on composite systems based on PVA, indicating their application focus on tissue engineering and regenerative medicine.

Chapter 4

4. DESIGN OF BIOACTIVE NANOFIBERS FOR TISSUE ENGINEERING

An important criticism of PVA fibers still concerns their poor cell adhesion properties, basically due to their lack of cell binding cues needed to promote more efficient cell recognition [130]. In the recent literature, several studies currently focused on using PVA blended with other biopolymers to improve biological and biomechanical properties [131], [132], [133], [134], [135]. Among them, gelatin—previously used as a gelling agent in some areas [136]— was offered as a bioactive agent to improve biocompatibility, promote cell interaction, and mimic the composition of fibrous components of the ECM. Furthermore, because gelatin has the RGD cell adhesive pattern, it influences the biological affinity and overcomes bioactivity limits [137]. Previous studies have demonstrated that structural proteins, like gelatin alone, exhibit poor workability to form electrospun nanofibers due to strong hydrogen bonding. At the same time, when in combination with other biopolymers, they can efficiently work firstly, by minimizing the jet instability phenomena able to promote the formation of beads along the fibers, and secondly, by improving polymer chain packing, with effects on the ultimate chemical and mechanical stability of the fibers [114], [138], [139]. Being a flexible material, gelatin can also be modified and processed with other materials for scaffolds used in nerve tissue engineering and other applications, thus broadening the scope of its use in the scaffolds [140]. Accordingly, structural proteins such as collagen, gelatin, or keratin have been combined with other synthetic polymers to fabricate electrospun scaffolds as ECM analogs [140], [141], [142], [143], [144].

The PVA/gelatin combination is an ideal material for electrospun nanofibers and is widely used in cell biology studies. Besides material properties, the morphology (i.e. fiber size, alignment) of electrospun nanofibers has an important influence on the morphology, adhesion and migration of cells. aligned electrospun nanofibers have been shown to be an important factor affecting the morphology and behaviour of cells. Astrocytes are cells sensitive to the orientation of fibers, and it is known that such oriented structures enable cells to organize in a certain direction and increase the functionality of the cells [145].

Astrocytes are the most abundant glial cells in the CNS and play a vital role in regulating a variety of critical neurological functions such as regulation of synaptic function, reuptake of neurotransmitters and neuroprotection. Furthermore, astrocytes contribute to the formation and maintenance of the blood-brain barrier, ensuring proper nutrient delivery and ion balance, which are vital for neuronal function [146]. In brain injuries and neurodegenerative diseases, astrocytes promote neural repair and regeneration. Understanding the dual roles of astrocytes in health and disease is crucial for developing therapeutic strategies targeting astrocytic functions in various neurological disorders [147]. Therefore, studying the behaviour of astrocytes is of great importance in neural tissue engineering.

Studies on biomaterials that affect the behaviour of astrocyte cells are critical for neural tissue engineering. However, there are no detailed studies investigating the effects of PVA/gelatin nanofibers and fiber orientation on the viability, adhesion and proliferation of astrocyte cells. The aim of this study was to investigate the effect of PVA/gelatin nanofiber scaffolds produced by electrospinning on the viability, proliferation and morphology of mouse astrocyte cells. Furthermore, how fiber orientation and gelatin content shape the cell behaviour of astrocytes will be investigated. This study aims to provide insights into the design of materials used in neural tissue engineering and better support of astrocyte cells.

4.1. Materials and Methods

PVA (Mw 130,000 Da, 99+% hydrolyzed), gelatin (type B from bovine skin), citric acid (ACS reagent, ≥99.5%), acetic acid (ACS reagent, ≥99.5%), ethanol, 1-ethyl-3-(3-dimethylaminopropyl) carbodiimide (EDC) and N-hydroxy succinimide (NHS), were all purchased from Sigma-Aldrich (St. Louis, MO, USA).

For the in vitro experiments, Trypsin-EDTA 1x, Dulbecco's Modified Eagle Medium (DMEM) High-Glucose, Fetal Bovine Serum (FBS) South America and Dulbecco's Phosphate-Buffer Saline (PBS) with and without Ca^{+2}/Mg^{+2} were all purchased from Euroclone (Pero, MI, Italy). DNase I, Alexa Fluor 488 Phalloidin, Alexa Fluor 594 donkey anti-rabbit IgG (H+L) and Alexa Fluor 647 donkey anti-mouse IgG (H+L) were all purchased from ThermoFisher Scientific (Waltham, MA, USA). Trypsin from porcine pancreas, Bovine Serum Albumin (BSA), Poly-D-Lysine (PdL) hydrobromide Mw 30-70kDa, and Mowiol 4-88, Anti-AQP4 antibody produced in rabbit (A5971), and Anti-GFAP antibody produced in mouse (G3898) were all purchased from Sigma-Aldrich (St. Louis, MO, USA).

4.1.1. PVA/Gelatin Solution Preparation

For the production of nanofibrous mats, PVA and gelatin were dissolved in acetic acid: water solution (1:2) as described before [148] with some modifications. Gelatin was preliminary dissolved in acetic acid at 50 °C (120 rpm for 1 h) and then mixed in PVA aqueous solution after cooling at room temperature. The final polymer concentration was kept of 10% (w/v) and the mass ratio between PVA and gelatin was varied as 50/50 and 70/30. For the control group, PVA solution was prepared with the 10% (w/v) concentration in water and heated to about 80 °C and stirred (120 rpm) for 3 h. Citric acid was also added to all the solutions before treatment to cross-link the PVA to maintain its structural integrity in aqueous media (10% w/w). Acetic acid was utilized with the gelatin solution to prevent gelation at room temperature [149].

4.1.2. Process Optimization and Post Processing

The plastic syringe with a 27G metallic needle was connected to a high-voltage power supply, used as the source of the electric field, into a grounded chamber containing an aluminium foil covered collector (NANON01; MECC, Fukuoka, Japan). It was placed into an additive syringe pump (KD Scientific, Holliston, MA, USA), vertically arranged with respect to the collector, to allow a controlled solution feed. An optimal set of process parameters was established in terms of voltage, flow rate, and electrode gap. The distance between the needle tip and the target was held constant at 25 cm. The voltage between the needle and target set as 19 kV. The flow rate of the polymer solution supplied to the syringe was fixed at 0.3 mL/h. A rotary drum collector system was used for aligned fiber production (700 rpm). All solutions were electrospun at room temperature under identical conditions for around 4 h, and relative humidity was kept at around 25%.

After the nanofiber production, samples were treated in the oven at 150°C for 15 min. In the case of the gelatin-filled samples, nanofibers were treated also with the EDC/NHS solution in order to prevent protein solubilization in water [150]. EDC/NHS/ethanol solutions (7.5 wt.%) were prepared with a ratio of EDC/NHS of 2/1 (w/w), added into ethanol ($V_{Ethanol}/V_{H2O}$ = 95/5) solution at room temperature, and stirred until complete dissolution was ensured. Nanofiber mats were placed into the crosslinking solution for 24 h, then rinsed with deionized water to remove the residual crosslinking solution and left to dry at room temperature for a further 24 h.

4.1.3. CHARACTERIZATION

4.1.3.1. MORPHOLOGY

A field-emission scanning electron microscope (Quanta FEG 200 FEI; Eindhoven, The Netherlands) with an accelerating voltage of 10 kV was used to evaluate the electrospun fibers' morphological features. Small pieces of membranes—rounded samples, 6 mm in diameter—were placed into the sputtering machine and coated with a Pd–Au nanolayer to improve surface electroconductivity—open-source image analysis software was used to measure average fiber diameters on selected SEM images (ImageJ 1.8; Fiji) and reported as mean value ± standard deviation (SD).

4.1.3.2. PHYSICAL AND CHEMICAL CHARACTERIZATION

FTIR Spectrum (PerkinElmer; Waltham, MA, USA) was performed from 650 to 4000 cm^{-1}.

4.1.3.3. IN VITRO STUDIES

ANIMALS

Wild-type (wt) pups with a CD1 genetic background were used for primary astrocyte cultures prepared as described below. Procedures involving animals were carried out in compliance with the European directive on animal use for research and Italian law on animal care. This project has been approved by the Italian Health Department (Approved Project no. n°710/2017-PR). The mice used here were bred in an approved facility at the University of Bari. Mice were kept under a 12h dark-to-light cycle, at constant temperature and humidity (22°C ± 2°C, 75%), with food and water ad libitum, and supplied with environmental enrichment materials such as toys and shelters. The experiments were designed to minimize the number of animals used and animal suffering.

MOUSE PRIMARY ASTROCYTES

Primary mouse astrocytes were prepared from neocortical tissues of 3-day-old mice pups as previously described [151]. Briefly, brains were extracted and cleaned of meninges and blood vessels, and the dissected neocortical tissues were incubated with 0.25% trypsin and 0.01% DNase in DMEM for 10 minutes at 37 °C. After addition of FBS to stop the trypsin, cells were washed with PB), passed through a 100 mesh and cultured in 25 ml cell culture flasks in DMEM High Glucose medium supplemented 10% FBS, 1% Penicillin/Streptomycin and maintained at 37°C in a 5% CO_2 incubator. After 7 days in culture, flasks were shaken with PBS without Ca^{2+}/Mg^{2+} to remove microglia and oligodendrocytes. Astrocytes were considered pure after two additional steps of trypsinization with Trypsin-EDTA 1x and replating.

CELL CULTURES

Nanofibrous materials were placed in non-adherent 24-multiwell culture plates and sterilized by incubation with 70% Ethanol in distilled water. Materials were then allowed to dry and washed with DMEM with 10% FBS and 1% Penicillin/Streptomycin, making use of the Phenol Red present in the media to make sure the materials have the proper pH. Media was aspirated and materials were allowed to dry at room temperature, after which cells were plated directly onto the materials using a minimum volume to keep the cells in the fibres. After 3 hours at 37 °C, the wells were filled with the appropriate amount of cell culture media. Controls were performed by plating cells onto glass coverslips treated with 10 µg/ml PdL for 20 minutes.

IMMUNOFLUORESCENCE

Nanofibrous materials and PdL treated coverslips were fixed in 4% paraformaldehyde, washed in PBS with Ca^{2+}/Mg^{2+}, and permeabilized with 0.3% Triton X-100 in PBS. After blocking with 2% BSA in PBS (PBS-BSA), cells were incubated with primary antibodies (rabbit anti-AQP4 and mouse anti-GFAP diluted 1:500 in PBS-BSA) for 1 h at room temperature. Cells were then washed three times with PBS with Ca^{2+}/Mg^{2+} and incubated with secondary antibodies and Phalloidin diluted 1:1000 in PBS-BSA for 1 hour. Cells were washed three times with PBS with Ca^{2+}/Mg^{2+}, after which coverslips were mounted directly on microscope slides and nanofibrous materials sandwiched in between a microscope slide and a coverslip, taking care to keep the seeded side facing the coverslip, using Mowiol 4-88, and examined by confocal microscopy (Leica TCS SP8).

4.1.3.4. STATISTICAL DATA

Experimental data were presented as the mean and standard deviation of each treatment. For in vitro assays, statistically significant differences, one-way analysis of variance (ANOVA), followed by Tukey's post hoc test ($p < 0.05$) were used.

4.2. RESULTS AND DISCUSSION

In tissue engineering, an effective regeneration needs a scaffold with appropriate biological and physical properties. As a result, several engineering and processing technologies have

been used to give the scaffolds the desired characteristics. Scaffolds made of synthetic polymers may have good mechanical and structural qualities, but they might not be the ideal for tissue ingrowth or cellular adhesion. Natural polymers have better biological qualities, but they lack physically strength and unstable in the physiological environment. As a result, using composite scaffolds made of both natural and synthetic materials blend is growing more popular [74]. Here, it was suggested to use gelatin to stimulate cell adhesion and development on nanofibrous scaffolds where PVA, a synthetic component, satisfies the necessary physical conditions.

Electrospun fibers were produced by electrospinning technique by a vertical deposition by using a flat collector for random fibers and rotating drum for aligned fibers. SEM micrographs of Figure 4.1 shows nonwoven nanofibrous mat structure produced from equal amounts of PVA/Gel solution via electrospinning process. The collected electrospun PVA/Gel mats were characterized by the absence of beads and exhibited a bimodal fiber distribution which is typical for bicomponent electrospun scaffolds. Mean diameters of neat PVA, PVA/Gel 7:3 and PVA/Gel 5:5 fibers were determined to be 0.924 ± 0.178 μm, 0.955 ± 0.146 μm and 0.599 ± 0.1 μm respectively. For the aligned samples, fiber size measured as 0.662 ± 0.204 μm. In the case of PVA/Gelatin blends, the 7:3 composition resulted in fibers larger and more uniform compared to the 5:5 composition. The molecular weight of dissolved material is an important parameter that reflects the solution viscosity. Higher solution viscosity is known to result in more uniform fibers with larger diameters [152]. The increased gelatin content in the 5:5 blend likely reduced the solution viscosity and introduced more variability in fiber formation, as evidenced by the higher standard deviation. This variability may be due to the structural and rheological differences between gelatin and PVA, leading to less stable jet formation during electrospinning. Thus, blending PVA with Gel, which consists of protein with a molecular weight lower than PVA, decreased the viscosity of solution though the total concentration was kept the same. Therefore, electrospinning of PVA/Gel solution formed nanofibers with a lower mean diameter than that of neat PVA.

For aligned fibers, the mean diameter was 0.662 ± 0.204 μm, comparable to the PVA/Gelatin 5:5 blend. However, the lower standard deviation in the aligned fibers indicates a more consistent fiber morphology. This homogeneity can be attributed to the alignment process, which may reduce variability in fiber formation by applying controlled electrostatic forces during electrospinning. Overall, the results indicate that higher gelatin content in PVA/Gelatin blends tends to produce thinner fibers but with increased heterogeneity. In contrast, alignment processes improve the consistency of fiber diameters, regardless of composition. From an application perspective, aligned fibers, with their thinner and more uniform diameters, may be advantageous for biomedical applications like cell growth or controlled drug release, where consistency in fiber size is critical. On the other hand, the PVA/Gelatin 5:5 blend, despite producing thinner fibers, exhibits greater variability in fiber diameters, as evidenced by the higher standard deviation, which might limit its utility in applications requiring precise structural uniformity. However, the smaller fiber diameters of the 5:5 blend may still offer potential benefits in applications where average size plays a more significant role than uniformity.

FIGURE 4.1: Morphological analysis of random fibers of a) PVA, b) PVA/GEL (7:3), c) PVA/GEL (5:5) and aligned fibers of d) PVA/GEL (7:3) e) PVA/GEL (5:5) and fiber size distribution graphs (scale bar: 50**μ**m). **This section is under embargo. The image has been removed and will be made available after the related article is published.**

Crosslinking is performed to maintain the structural integrity of PVA and gelatin in aqueous media. Citric acid is a non-toxic substance that has been successfully used in PVA

crosslinking. For gelatin, EDC NHS is preferred over toxic aldehyde-based crosslinkers. In this study, a combination of the two was used and the samples were subjected to a stability test lasting 24 hours. Figure 4.2 shows the SEM imaging of the samples prepared using different crosslinking methods after 4 hours and 24 hours in PBS at 37°C. In the images, it was observed that crosslinking using a single method caused problems in fiber morphology and disrupted pore structures. Especially in the method using only CA, it is seen that gelatin cannot remain stable in the PVA structure and covers the surface and closes the pores. Since pore structure and fiber morphology are important factors in tissue engineering applications, it was deemed appropriate to continue the study with materials created using both methods.

FIGURE 4.2: SEM pictures show the stability test results after different crosslinking methods were applied to randomly collected PVA/Gel (7:3) samples. The combination of two methods (Citric acid + EDC/NHS) was used by first heat treating the citric acid added sample and then adding EDC/NHS and washing. **This section is under embargo. The image has been removed and will be made available after the related article is published.**

FTIR analysis was also conducted to obtain further indications regarding the chemical composition of the fibers and interactions also to evaluate the presence of gelatin in the fibers. Figure 4.3 demonstrate the chemical structure and stabilization of PVA/Gel nanofibers before and after different crosslinking methods. These results are particularly significant for evaluating gelatin presence and the stability of the fibers for biomedical applications. As seen in the upper graph, in the citric acid (CA) crosslinked fibers, the

characteristic peaks of gelatin at 1647 cm^{-1} (Amide I; C=O stretching) and 1539 cm^{-1} (Amide II; N-H bending and C-N stretching) are clearly identifiable. Additionally, the CA crosslinking introduces a peak around 1710 cm^{-1}, corresponding to C=O stretching of ester groups, indicating a reaction between the carboxyl groups of citric acid and the hydroxyl groups of PVA. However, fibers crosslinked with only CA exhibit limited structural stability as seen also SEM figures. In the EDC/NHS crosslinked fibers, the gelatin-specific Amide I and II peaks are preserved, and this method, targeting the protein amine groups, enhances fiber stability. When both crosslinking methods (Citric acid + EDC/NHS) are applied, the spectra show both the characteristic gelatin peaks and the ester group peak, confirming the dual crosslinking's ability to maintain gelatin's chemical stability and improve fiber morphology. In contrast, uncrosslinked fibers exhibit the presence of gelatin, but their lack of stabilization leads to rapid degradation in aqueous environments.

In the lower graph, which depicts the results after a 24-hour stabilization test in PBS, the dual crosslinked fibers (Citric acid + EDC/NHS) retain their morphology and porosity, with the FTIR spectrum still showing the Amide I and II peaks of gelatin. In comparison, fibers crosslinked with a single method show partial gelatin loss or structural alteration due to insufficient stabilization.

.

FIGURE 4.3: Comparison of crosslinking methods of PVA/Gel; a) non-crosslinked (wo CL), EDCNHS crosslinked (ENCL), Citric Acid crosslinked (CACL) and Citric Acid + EDCNHS both crosslinked (bothCL). b) PVA/Gelatin crosslinked with citric acid + EDCNHS and after 24h in PBS. **This section is under embargo. The image has been removed and will be made available after the related article is published.**

Primary mouse astrocytes were seeded on PVA and PVA/Gel materials. Cells exhibit minimal interactions with their surrounding matrix when cultured in PVA, while those cultured in PVA/Gel nanofibers show more isotropic and elongated morphologies (Figure 4.4). To study how the disposition of nanofibers affected cell-material interactions, we seeded cells in both aligned and non-aligned nanofibrous materials. We observed how cells cultured in aligned nanofibers exhibit much more elongated morphologies, with a much higher confluence after 7 days in vitro when compared with the randomly deposed fibers.

FIGURE 4.4: Representative fluorescence microscopy images of primary mouse astrocytes on PVA and PVA-GEL nanofibers. PVA(top), not aligned (middle), aligned (bottom), PVA/GEL 50:50 (left) PVA/GEL 70:30 (right). F-actin is stained by phalloidin-488 (green). Scale bars are 100 μm. **This section is under embargo. The image has been removed and will be made available after the related article is published.**

To further study these cell's morphology, we performed high resolution confocal microscopy images staining for F-Actin and astrocyte markers Aquaporin 4 (AQP-4), an active water channel protein, and glial fibrillary acidic protein (GFAP) (Figure 4.5). In this resolution, it becomes clear how the cells in the aligned materials adopt a much more elongated morphology, aligning themselves with the material fibers, with respect to the ones cultured in the non-aligned fibers.

FIGURE 4.5: Confocal microscopy images and 3D reconstruction of primary mouse astrocytes cultured in PdL treated coverslips, PVA, and both aligned and not aligned PVA/Gel 50:50 and 70:30. Vertical view (top) and horizontal view (bottom) with material side down. F-Actin is stained by Alexa Fluor 488 Phalloidin (green), AQP-4 is stained by Alexa Fluor 594 (red) and GFAP is stained by Alexa Fluor 647 (blue). Scale bars are 15 μm. **This section is under embargo. The image has been removed and will be made available after the related article is published.**

The incorporation of gelatin into PVA nanofibers significantly enhanced cell adhesion and morphological changes compared to pure PVA. Due to its unique properties in gelatin, including the presence of the RGD sequence, a cell recognition motif found in various ECM proteins, it interacts with integrin receptors on the cell surface to promote cell attachment and mediate cell adhesion. In addition, it forms a scaffold that supports astrocyte viability and growth, complementing the mechanical strength of PVA. The dual crosslinking method using citric acid and EDC/NHS was shown by SEM analysis to maintain the structural integrity and porosity of PVA/Gelatin scaffolds under physiological conditions. The single-method crosslinking led to morphological disruptions, such as pore closure and altered fiber morphology. The optimized crosslinking approach maintained the fibrous architecture necessary for tissue engineering applications, ensuring that the scaffold remains stable during cell culture. Besides, FTIR analysis confirmed the successful integration of gelatin within the PVA structure, with amide I and II peaks indicating the presence of proteins critical for cell-matrix interactions and still present after crosslinking.

The observed elongation and isotropic morphology of astrocytes cultured on PVA/gelatin fibers suggest that this composite material provides a more biocompatible environment compared to synthetic PVA alone. In particular, the elongated morphology observed on aligned nanofibers highlights the role of topographical cues in directing astrocyte organization. While this behavior contrasts with the isotropic elongation typically seen on PdL-coated substrates, it demonstrates the ability of astrocytes to respond to scaffold alignment, which may influence cellular interactions and functionality in neural tissue engineering applications. Conversely, random fibers led to less organized cell morphology, emphasizing the importance of tailoring scaffold architecture to specific cellular requirements.

4.3. CONCLUSION

This chapter emphasizes the significance of material functionalization, fiber orientation, and crosslinking techniques when fabricating nanofibrous scaffolds for the repair of neurological tissue. The PVA/gelatin nanofibrous scaffolds developed in this study exhibited promising results towards enhancing both the adhesion and proliferation of astrocytes. This merely highlights the prospects of using a hybrid of natural and synthetic polymers in preparing bioactive materials in order to bio replicate the extracellular matrix while maintaining the necessary structural and mechanical characteristics.

The application of the dual crosslinking method using citric acid together with EDC/NHS appears to be a major factor in the retention of the structural integrity and porosity of the scaffolds when placed in water. This optimized strategy was found to be more effective than using the single method crosslinking, in that it enhanced the fibrous architecture critical to tissue engineering applications. FTIR analysis showed that after crosslinking the expected gelatin incorporation into the PVA matrix was observed with Amide I and II peaks showing crosslinked gelatin doped with its bioactive elements. The roles and effects of dual crosslinking in improving and maintaining fiber morphology and pore structures which ensure cellular activity and nutrient interchange were also confirmed through SEM imaging.

In conclusion, this study investigated the composition and the process of designing and making PVA/gelatin nanofibrous scaffolds for the neural tissue engineering use. The key reason for polymer blending of PVA's strength and gelatin's biocompatibility composition is to provide optimal conditions for growth and functioning of astrocytes. The findings presented will provide a basis for the development of more sophisticated techniques for neural tissue reconstruction and recovery, which may find application in the treatment of neurological diseases, brain trauma, or degeneration processes. In this way, other lines of research that may be promising include scaling up production, investigation of optimization of the scaffold fabrication process, and examination of bioactive agent or growth factor additive effects to scaffolds to enhance their therapeutic effects more.

Chapter 5

5. DESIGN OF ELECTROACTIVE NANOFIBERS FOR TISSUE ENGINEERING

The creation of electroactive nanofibers has stood out as an important area of interest in tissue engineering and regenerative medicine, as these fibers are able to replicate the electrical characteristics found in biological tissues. These fibers participate in electrical signaling within tissues like muscle and nerve as well as in cellular events including adhesion, proliferation, and differentiation. Electroactive fibers are able to achieve improvement in cell material interactions by offering both nanometer scale roughness and electrically conductive properties, which in turn results in improvement in tissue repair and regeneration. Recent developments in the incorporation of conductive materials with bio-degradable polymers have widened the scope of applications of electroactive fibers from tissue engineering scaffolds to advanced biosensors. In this chapter, the MXenes are proposed as a new technological solution to improve the electroactive properties of nanofibers.

MXenes have received wide interest owing to their high electrical conductivity, hydrophilicity, excellent mechanical properties, and biocompatibility. These characteristics make MXenes an appropriate material for a variety of biological applications, ranging from tissue engineering to drug delivery and biosensors. MXenes combined with hydrogels and biodegradable polymers gave rise to materials with high chemical activity and flexibility, which are critical parameters for several biomedical applications. Research has shown that tissue regeneration can be achieved using MXene, specifically supporting rapid bone regeneration and providing antibacterial signals necessary for wound healing [153], [154]. In the literature, there are various studies on different materials developed using MXene

and PVA. The electrical, mechanical and biological properties of MXene and the biocompatibility and hydrophilic properties of PVA have enabled the combination of these two materials to be used in many different applications. A study has shown that MXene/PVA/n-HA composite had significantly enhanced mechanical properties, bioactivity, and good osteogenic properties. Specifically, the addition of 2% MXene by weight was found to optimize these attributes, making the composite membranes ideal candidates for applications like guided bone regeneration [155].

Thus, electrospinning technology for the production of nanoscale fibers is distinguished by its versatility. The new development of MXene fibers led to the creation of ultra-compact high performance fibers characterized by excellent electrical conductivity, strength and toughness. With such features, the fibers have potential uses in textiles including EM shielding and electrothermal effects [156].

Currently, the development of new methods for fabricating freestanding films with minimal inactive components has increased the demand for lightweight and flexible systems with high conductivity. $Ti_3C_2T_x$/PVA and $Ti_3C_2T_x$/Cellulose Nanocrystals/PVA composite nanofibers with improved mechanical and electrical properties were prepared [157]. Hence, the integration of MXenes into nanofibers is valuable for tissue engineering and other biomedical applications and has emerged as an emerging research area [158]. In recent studies, different uses of MXenes and PVA separately, as well as their combined forms, have been investigated [159], [160], [161]. Over the last ten years, PVA with specific hydrophilic characteristics and the capacity to create membranes or gels has been fused with organic (gelatin) or inorganic components like as metal ions and bioactive glasses in numerous ways to improve mechanical properties and bioactivity [162], [163]. From this perspective, the incorporation of conductive elements like MXenes can also improve the functional properties - mainly the electrical and mechanical properties - possibly broadening the scope of their usage in wound healing, medical devices, and tissue engineering.

In this chapter, the optimization of composite fibers is proposed through the combination of $Ti_3C_2T_x$ inks and nanometric fibers drawn from an aqueous PVA solution, the aim here being to obtain electrospun MXene loaded PVA fibers with improved properties through the modification of electrospinning parameters. This underscores the applications envisaged for them in biomedicine and the fact that there remains a need for more investigation in order to improve their performance in different biomedical settings. The biocompatibility and bioactivity of the optimized fibers were investigated to evaluate their suitability for use in cell adhesion, proliferation, and differentiation which are important parameters in tissue engineering. Finally, the knowledge acquired during this research would possibly assist in coming up with improved biomedical materials with better functionality and enhanced performance.

5.1. Materials and Methods

5.1.1. PVA/MXene Solution Preparation

PVA aqueous solution was prepared at 16% (w/v), heated to 80 °C, and stirred (120 rpm) for 3 hours. After cooling to room temperature, $Ti_3C_2T_x$ MXene at a concentration of 5 mg/ml was mixed into the PVA aqueous solution and stirred at 120 rpm for 1 hour to obtain a PVA/MXene composite with final concentrations of 10% and 0.2% (w/v), respectively (Figure 5.1). Electrospun nanofibers were fabricated using a vertically arranged electrospinning (NANON01; MECC, Fukuoka, Japan).

5.1.2. Process Optimization

5 mL of the PVA/MXene mixture was loaded into a 5 mL syringe equipped with a 27G metallic needle. The syringe was connected to an additive syringe pump (KD Scientific, Holliston, MA, USA) to allow controlled solution feeding. The electrospinning process was carried out at room temperature with a voltage of 20 kV, a flow rate of 0.3 mL/h, and 25 cm between the needle tip and the collector. The fibers were collected for 1 hour.

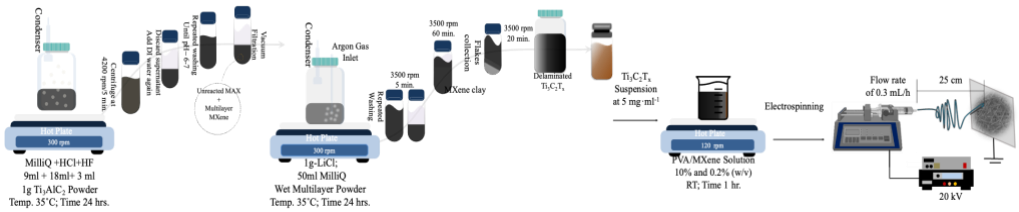

FIGURE 5.1: Scheme of MXene preparation and electrospinning process of PVA/MXene [10]

5.1.3. CHARACTERIZATION

A field-emission scanning electron microscope (FE-SEM, Quanta FEG 200, FEI; Eindhoven, The Netherlands) with an accelerating voltage of 10 kV was used to evaluate the morphological features of the electrospun fibers. Small pieces of membranes—rounded samples, 6 mm in diameter—were placed into the sputtering machine and coated with a Pd–Au nanolayer to improve surface conductivity. Open-source image analysis software (ImageJ 1.8; Fiji) was used to measure the average fiber diameters on selected SEM images.

To analyse the surface elemental composition of the fibers in terms of weight and atomic percentages, Energy Dispersive X-Ray Spectroscopy (EDS) was conducted. FTIR Spectrum (PerkinElmer; Waltham, MA, USA) was performed from 650 to 4000 cm^{-1}.

Wide angle X-ray scattering measurements (WAXS) were collected at room temperature with a PANalytical Empyrean diffractometer operating in reflection geometry (θ−θ scans, with 2θ the scattering angle) using a Ni-filtered Cu-Kα radiation (λ = 1.5418 Å).

Electrical properties were assessed by depositing 1 µm thick films made of pure PVA and PVA/MXene fibers on multilayer substrates consisting of a 500 µm thick highly doped silicon (Si^{++}), a 200 nm thick SiO_2 dielectric barrier, and 150 nm thick pre-patterned interdigitated gold electrodes. Before film deposition, the SiO_2 surface was cleaned in ultrasonic baths of acetone and isopropanol, then dried by nitrogen gas. For all samples, four active channels were achieved with two different pairs having length (L) of 20 and 40 um, respectively. The channel width (W) was scaled so that the ratio between W and L was invariably 550. This layout has been previously employed to reliably assess the

conductivity and mobility performances of a wide range of organic and inorganic compounds [164]. For the electrical tests, the samples were contacted using a Signatone probe station, equipped with micro-manipulators bearing metallic tips, connected to a Keithley 2612A dual channel source-meter. Using this experimental setup, the background current noise level was approximately 0.1 nA.

Mechanical tensile tests were carried out using the Instron dynamometer 5566 (Instron, Bucks, UK) equipped with a 10 N loading cell. Dog bone shaped specimens were obtained through the Ceast cutting machine equipped with an ASTM D1708 cutting die. The non-contact laser sensor (Micro-Epsilon optoNCDT 1420-10, MICRO-EPSILON UK & Ireland Ltd., Ortenburg, Germany) was used for measuring specimens' thickness. Each specimen was clamped on the dynamometric equipment through titanium chucks, a preload of 0.01 N was applied before running the tensile test at an elongation speed of 1.0 mm/min up to rupture. Force and elongation data were acquired at a speed of 10 pts/s. Stress and strain were obtained by dividing the load and the elongation by the specimen's cross-section area and the initial length, respectively. Mechanical properties (i.e. Young's modulus, maximum stress and maximum strain) were detected on stress vs strain diagrams. Analysis of variance was performed at a probability level $p = 0.05$ using the OriginPro 2018 software (OriginLab Corporation, Northampton, USA).

To evaluate the biological influence of MXene on the PVA fibers, L929 cells (fibroblasts derived from mouse, Sigma-Aldrich, St. Louis, MO, USA) were used to perform Cell Proliferation Kit II (XTT assay, Roche Diagnostics Deutschland GmbH, Mannheim, Germany, purchased by Sigma-Aldrich). This assay indicates cell viability based on the metabolic activity of living cells. Firstly, L929 cells were cultured in DMEM (Sigma Aldrich, Milan, Italy) containing 2 mM of L-glutamine (Sigma-Aldrich, Milan, Italy), 10% FBS (Sigma-Aldrich, St. Louis, MO, USA), and 1% antibiotic solution (streptomycin 100 µg/mL and penicillin 100 U/mL, Sigma-Aldrich, Milan, Italy). The cells were incubated at 37°C with 5% CO_2. Before the in vitro assay, samples were cut, placed into a 96-well cell culture plate, and sterilized with a solution of 70% ethanol. The samples were then washed with PBS, (Sigma Aldrich, Milan, Italy) and dried under a hood. For biocompatibility tests, a

density of $1x10^4$ cells per well was seeded onto the PVA and PVA/MXene fibers. The XTT assay was conducted according to the manufacture's protocol after 1, 3, and 7 days in cell culture. Briefly, the cell culture media was removed and replaced with fresh culture media containing XTT reagent and incubated for 4 hours under standard conditions. After that period, the supernatant from each well was collected and placed into a 96-well plate reader to measure the absorbance at 450 nm using a spectrophotometer (Wallac Victor 1420, PerkinElmer, Boston, MA, USA).

5.2. Results and Discussion

Recent studies have focused on the idea that regenerative processes can be supported and accelerated by electrical stimuli which can facilitate the repair of the injured tissues. For this purpose, the use of intrinsically electroconductive polymers is rapidly growing for different biomedical applications, from medicine to biosensing. In this view, the fabrication of PVA fibers by integrating material phases with different electroconductive properties was preliminarily investigated.

A solution of PVA and MXene was employed to fabricate electrospun nanofibers. The average diameter of electrospun fibers is a crucial parameter that significantly influences various applications relying on size-dependent properties, such as tissue engineering and sensor technologies [165]. Scanning Electron Microscopy (SEM) was used to examine the impact of MXene addition on fiber diameter distribution. SEM micrographs of the composite nanofibers are presented in Figure 5.2**.** The nanofibers appear smooth without beads, with diameters of 696 ± 160 nm for PVA and 587 ± 191 nm for PVA/MXene. The reduced fiber diameter could be attributed to the strong polar interactions of MXene into the solution that enhanced jet stability during electrospinning. In detail, MXene particles tend to interact with water molecules in solution promoting their intercalation into the polymer solution with an overall stretching effect on the polymer jet. This effect tends to enhance the mechanism of solvent evaporation thus favoring a slight reduction of the ultimate diameter of the fibers, preserving a good uniformity of particles dispersion into the fiber bulk, in agreement with previous similar studies [166], [167]. However, MXene

concentrations above the optimal concentration can negatively affect the jet stability in the electrospinning process by increasing the viscosity in the solution. Besides, it can reduce the suitability of nanofibers for tissue engineering applications since the lower ratios are known to provide an ideal balance. PCL nanofibers loaded with MXene (up to 0.5 wt%) are known to show greater biocompatibility compared to structures embedded with higher MXene ratios [168].

The presence of MXene within the electrospun nanofibers was confirmed by detecting the Ti element in the EDS spectra (Figure 5.2 d), consistent with earlier reports [169]. The spectrum analysis provided a detailed breakdown of the elemental composition, with weight and atomic percentages of titanium recorded at 0.54% and 0.19%, respectively.

The FTIR spectra of PVA and PVA/MXene are shown in Fig 5.2e, covering the frequency range of 4000–650 cm^{-1}. The spectra display almost identical peaks with slight shifts, indicating primarily physical interactions between PVA and MXene nanoparticles. The main absorption peaks for PVA and PVA/MXene occur around 3277 cm^{-1} (O-H stretching), 2909 cm^{-1} (C-H stretching), 1420 cm^{-1} (CH_2 bending), 1088 cm^{-1} (C–O–C stretch), and 911 cm^{-1} [170]. However, shifted stretching of pure PVA at 3274 cm^{-1} and at 832 cm^{-1} likely result from MXene's surface functional groups interacting with PVA and altering the vibrational properties of the polymer matrix [171], [172], [173]. The comparison of these spectra indicates the successful integration of MXene into the PVA matrix, leading to modified vibrational characteristics.

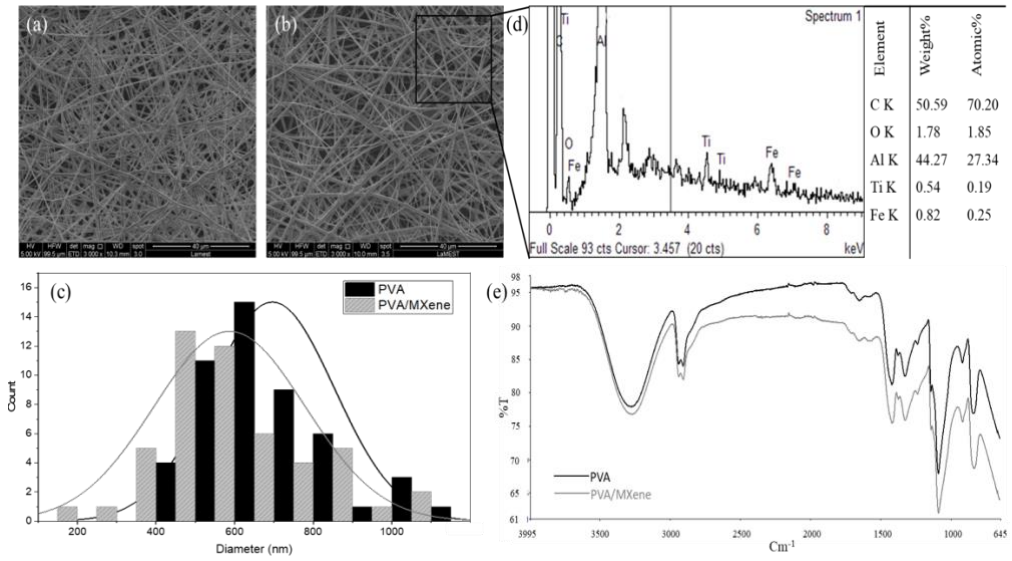

Figure 5.2: SEM micrographs of electrospun nanofibers: a) PVA, b) PVA/MXene (Scale bar: 40µm). c) Fiber diameter distribution for PVA (black) and PVA/MXene (grey). d) EDS spectrum and weight and atomic percentage of elements. e) FTIR analysis of PVA (black) and PVA/MXene (grey) [10].

The electrical properties of the investigated films, deposited on Si^{++}/SiO_2 substrates equipped with gold electrodes (Fig. 5.3 a, b), were assessed in air by performing two-probe current-voltage (IV) measurements. The applied voltage was swept from 0 to + 30 V and then backward to highlight any possible hysteretic effects. The voltage step was fixed at 200 mV with an overall scan rate of 1 V/sec. Fig. 5.3 c (left panel) shows two IV traces recorded for PVA/MXene active channels. These curves exhibit a clockwise hysteresis, indicating that the current values acquired during the forward scan (from 0 to 30V) were larger than those recorded during the backward scan (from 30 to 0 V). This behavior is typical of many non-crystalline conducting systems and is mainly associated to charge trapping mechanisms, which tend to immobilize carriers during the measurement acquisition [174]. Fig. 5.3 c (right panel) presents a direct comparison between a set of IV curves measured for devices based on PVA/MXene and pure PVA fibers. This plot makes clear that the integration of MXene flakes in the PVA fibers tend to enhance the electrical properties in comparison with the pure PVA system.

In Fig. 5.3 d we detail the forward scan of an IV curve recorded for a PVA/MXene active channel. While the current exhibits a diode-like (sub-linear) behavior in the low voltage region, indicating the presence of non-ideal charge injection mechanisms, it follows a linear behavior when the applied voltage exceeds 10 V. This latter region was used to extract the conductivity (σ) values by fitting the measurement linearly based on Ohm's law. In Fig. 5.3 e, the average conductivity values estimated for PVA/MXene and pure PVA fibers are plotted with error bars representing the standard deviations. The MXene integration in PVA fibers resulted in a fourfold increase in conductivity (σ = (1.90 +/- 0.45) $\cdot 10^{-8}$ S/cm) compared to the pure PVA system (σ = (0.46 +/- 0.05) $\cdot 10^{-8}$ S/cm).

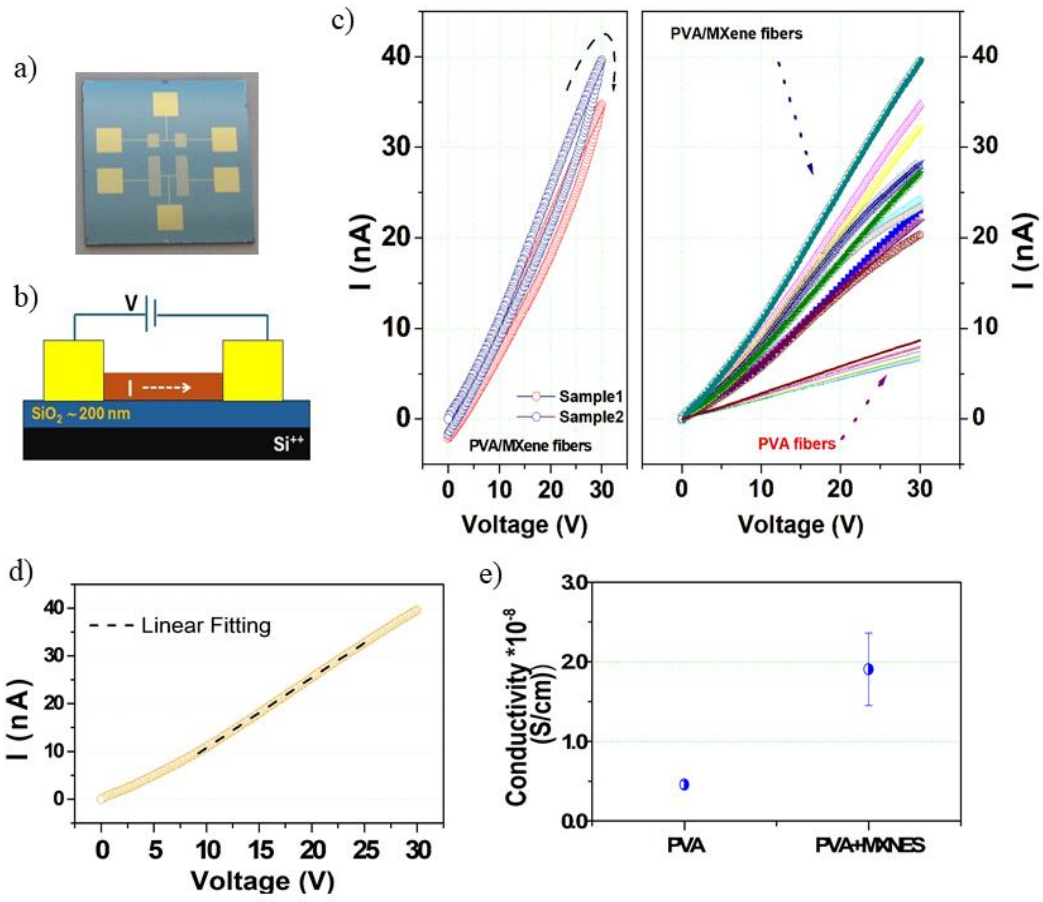

FIGURE 5.3: a) Top view and b) schematic side view of the device layout used for the electrical tests. c) (left panel) two IV curves acquired for PVA/MXene active channels; (right panel) comparison between a set of IV curves recorded for PVA/MXene and pure PVA samples. d) the linear fitting curve used to estimate the conductivity values of a PVA/MXene active channel. e) comparison of the average conductivity values estimated for pure PVA and PVA/MXene fibers. Error bars represent the standard deviations [10].

Typical stress vs strain curves for PVA and PVA/MXene were shown in Fig. 5.4 a. Both materials presented a maximum point before fracturing located at an elongation of about 50% and 200% for PVA/MXene and PVA, respectively. Fig. 5.4 b, c showed the stretching occurring during the tensile test for PVA and PVA/MXene, respectively. While PVA

continuously elongates reducing its cross-section area up to rupture (Fig. 5.4 b), PVA/MXene displayed a cross-section reduction up to a lower elongation level as a crack started to slowly propagate through the specimen (Fig. 5.4 c)

Mechanical properties of PVA and PVA/MXene samples were computed through the stress vs strain diagrams, and they were reported in Fig. 5.4 d-f. The incorporation of MXene nanoparticles into PVA significantly improved both stiffness and strength of PVA (Fig. 5 d, e, respectively), however a significant decrease in ductility was observed (Fig. 5.4 f).

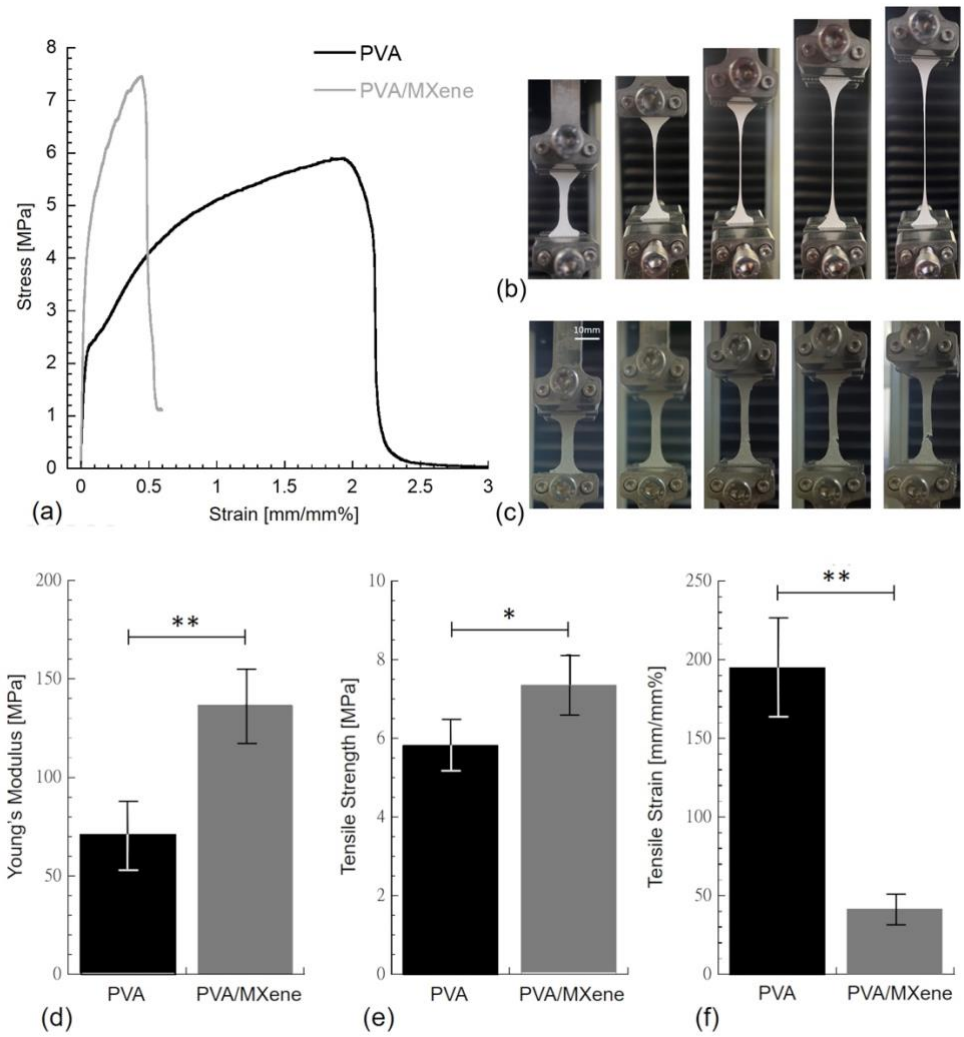

FIGURE 5.4: Tensile test. a) Typical stress vs strain curves for PVA and PVA/MXene; stretching occurring during the tensile test for b) PVA and for c) PVA/MXene specimens; mechanical properties of PVA and PVA/MXene in terms of d) Young's modulus e) Tensile strength f) Maximum strain occurring at the maximum stress. Error bars represented the standard deviation, while significant differences were indicated as * ($p<0.05$) and ** ($p<0.01$) [10].

Young's modulus (i.e. the stiffness) of PVA (71.42 ± 16.56 MPa) was significantly lower ($p<0.01$) than that of PVA/MXene (136.87 ± 19.63 MPa). Mean Young's modulus measured

for PVA was consistent with values reported in the literature [175], [176], while a similar stiffness increases of about 90% was also reported for the storage modulus at room temperature as MXene was incorporated into PVA [177].

Tensile strength of PVA/MXene (7.35 ± 0.78 MPa) was significantly higher ($p < 0.05$) than that of PVA (5.34 ± 0.67 MPa). Tensile strength mean value measured for PVA was consistent with those reported in the literature [178], [179], but higher strength values for PVA were also recorded [180]. The above results suggest that the incorporation of MXene nanoparticles into PVA effectively increased the strength by acting as a reinforcement agent, however the stiffness increase of about 90% suggested that MXene increased cross-linking density. Maximum strain (i.e. ductility) of PVA/MXene (41.31 ± 9.69 mm/mm %) was significantly lower ($p < 0.01$) that that of PVA (194.87 ± 31.43 mm/mm %). Maximum strain recorded for PVA is consistent with maximum strain values reported in the literature [181], [182], and similar ductility reduction were observed as chitosan nanoparticles were incorporated into PVA [183].

To evaluate in vitro biocompatibility, L929 fibroblasts were used (Fig. 5.5). The viability of cells seeded onto PVA and PVA/MXene fibers were similar at 1 and 3 days for all samples. This effect can be attributed to the high hydrophilicity of PVA [184], [185] as previously reported in similar studies addressing various biomedical applications such as wound dressing, tissue regeneration, and drug delivery [186], [187], [188]. Moreover, the surface groups such as hydroxyl, oxygen, or fluorine on MXene enhance its hydrophilic properties [189], [190], further supporting protein adsorption onto the fiber surface and ultimately promoting cell adhesion. In vitro tests showed an increase in metabolic activity from 3 to 7 days, consistent with previous experimental studies [191]. Notably, a more gradual increase was observed in the case of PVA/MXene fibers, while a significant rise in viability was detected at 7 days for PVA fibers. These preliminary findings will be foundational for future biological studies aimed at in vitro validation of the electrical properties of PVA/MXene fibers and their effects on cell proliferation and differentiation [192]. This research is particularly relevant for mimicking the unique microenvironment of electroactive tissues such as muscle and neural tissue.

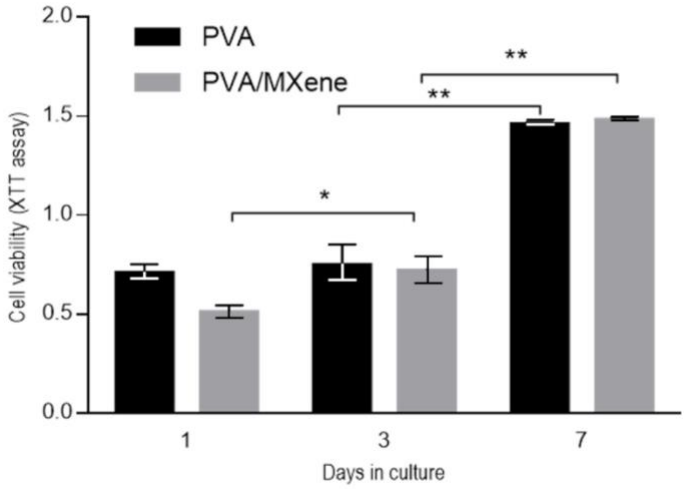

FIGURE 5.5: Cell viability of L929 fibroblasts seeded onto PVA and PVA/MXene fibers. An increase in absorbance is directly correlated with the number of living cells. Results are presented as mean ± standard deviation of the XTT absorbance. Significant differences are indicated as *$p < 0.05$; **$p < 0.01$ [10].

5.3. CONCLUSION

To date, few studies have been conducted on /PVA/MXene-based materials. These studies indicate that PVA/MXene materials can be applied in diverse application areas, as a function of specific properties exerted by the materials in different forms (e.g., film, gels). In this study, MXene-incorporated PVA nanofibers were prepared by electrospinning, and their structural, electrical, and biological characteristics have been optimized for the development of smart devices for wearable/flexible bioelectronics. The conductivity of the nanofibers was increased four times because of MXene doping, and the mechanical properties were doubled. Moreover, in vitro tests confirmed that MXene-containing PVA nanofibers are not toxic for fibroblasts, also enhancing cell growth. Despite other in vitro tests have been performed on MXene-loaded systems, no positive effects had been reported in terms of cells/material interaction. Accordingly, peculiar morphological signals of PVA/MXene nanofibers with high surface to volume ratios contributed to improve the

biological mechanisms at the cell interface, in comparison with other substrates (i.e., film, gels). Moreover, their peculiar architecture with homogeneously distributed pores embedded into a highly repeatable texture also concur to particularize mechanical and electrical properties for different biomedical and engineering applications. In this view, further investigation on the ability to tune electrical conductivity by the application of different mechanical forces will be required to quantitatively evaluate the actuation mechanisms regulating the biosensing properties of the proposed systems for the fabrication of electro-actuated patches to be included into high performance, medical and/or military wears.

Chapter 6

6. EFDT APPLICATIONS FOR DRUG DELIVERY SYSTEMS

EFDTs, such as electrospinning and electrospraying, are becoming more common and popular with variations and possibilities for utilizing them in creating novel drug delivery systems. These technologies enable the construction of nanofibers and microgels with the desired dimensions, shapes, and structural particulars, thus, optimizing for the encapsulation and release of therapeutic agents. Due to the high surface area to volume ratio nanofibers have been found to be useful in drug loading and prolonged drug release delivery systems whilst electro-spraying microgels with core shell structures can be used for the controlled and regional release of drugs [193], [194], [195].

Drug-nanofiber composites are known to have the ability to deliver drugs more locally and are thus employed in wound healing as well as in the scaffolds used in tissue engineering. Drug nanofibers have a fibrous composition which works as a three-dimensional framework that allows the growth of cells while ensuring the gradual release of biologically active compounds [196]. Conversely drug loaded microgels are envisaged to have high possibility of systemically targeted and aimed delivery to such organelles such as nuclear materials and to organs or tissues in the body [197].

This chapter considers the use of EFDT in the construction of drug-loaded nanofibers and microgels with a focus on their design, optimization and evaluation for drug delivery. The introduction of such systems in biomedical applications substantiates their ability to enhance therapeutic outcome, lower adverse effects, and contribute towards precision medicine.

6.1. DRUG LOADED NANOFIBERS

In this work, PCL was used as a replacement for PVA in drug delivery systems. PCL is a synthetic polyester that has a good biocompatibility, is capable of biodegradation, and has mechanical stability which is beneficial for long-lasting drug release systems. PVA, on the other hand, is water soluble and hydrophilic whereas PCL is hydrophobic and hence this increases the rate of degradation to be more gradual. This particular property is especially advantageous for drug delivering systems that are expected to be active for a long time. In addition, PCL has crystalline structure and thermal stability which serves to reinforce the scaffold, making it ideal for scenarios where mechanical properties are crucial. The focus of this chapter is thus directed at enhancing the encapsulation and release characteristics of therapeutic agents in electrospun nanofibers by using PCL with the objective of optimizing drug delivery attributes for biomedical devices.

6.1.1. MATERIALS AND METHODS

PCL (0.4 g) and gelatin (0.4 g) were dissolved in 4 mL of hexafluoroisopropanol (HFIP). To investigate the effect of solvents on drug release behavior, various ratios of acetic acid and water were added to HFIP as co-solvents. Diclofenac sodium (0.04 g) was incorporated into the PCL/Gel solution as the model drug. The resulting mixture was stirred until a homogeneous solution was obtained and then processed using electrospinning to fabricate drug-loaded nanofibers. Electrospinning was conducted for 5 hours with the following parameters: flow rate of 0.1 mL/h, applied voltage of 13 kV, and a collector-to-needle distance of 15 cm.

Fiber yield was gravimetrically obtained from the entire mass of fiber recovered. Encapsulation efficiency and drug release profiles were evaluated for different diclofenac sodium (DicNa)-loaded nanofibers. Briefly, samples with a known mass were dissolved in 1 mL of TFA, and the solution was added dropwise to 20 mL of methanol, in which the polymer was precipitated and DicNa was dissolved for 4 h. After centrifugation at 4000 rpm for 10 min at 4 °C (Eppendorf Centrifuge 5702 R, Hamburg, Germany) of the methanol solution, the liquid supernatant was collected, and DicNa was quantified by

spectrophotometric assay (UV-1800; Shimadzu Laboratory World, Tokyo, Japan) at λ = 323 nm. A calibration curve calculated the amount of DicNa in a concentration range of 0.5–50 mg/mL (y = 0.0184x + 0.0251, R_2 > 0.998). The encapsulation efficiency EE% was calculated by Equation (1):

$$EE\% = 100 \cdot (C_e / C_T) \quad (1)$$

where C_e is the amount of entrapped drug in the nanofibers and C_T is the total amount of the drug used to prepare the nanofibers. The results were recorded as average ± standard deviation for at least three independent batches.

The release of DicNa from PD and PGD nanofibers was evaluated by initially immersing the samples in 30 mL of PBS buffer solution at pH 7.4. They were then placed in a thermostatic incubator set to shake at 100 rpm and 37 °C. At designated time intervals, 1 mL of the release medium was withdrawn and replaced with an equivalent volume of fresh medium. The concentration of DicNa in PBS was assessed over a range of 0.2–50 mg/mL. For this purpose, a calibration curve was established using a series of DicNa solutions with standard concentrations and measured at a wavelength of 280 nm, resulting in the equation y = 0.0357x + 0.0175, with an R^2 value of 0.9969.

6.1.2. Results and Discussions

The release rates of DicNa from PCL/gelatin nanofibers formed with different solvents were evaluated so as to examine their drug delivery capability. Four formulations being A25, A50, W25, and W50 were prepared in which every solution has different amount of acetic acid (A) or water (W) that was added together with HFIP. In this case, A25 and A50 have 25% and 50 % volume of acetic acid with HFIP whereas W25 and W50 have 25 % and 50 % volume of water with HFIP respectively.

The SEM and fiber diameter measurements were evaluated and indicated that the solvent composition has an impact on fiber morphology (Fig 6.1). Control sample (HFIP) kept the

largest average fiber diameter measured at (0.6 ± 0.08 µm) and demonstrated the least variance suggesting that there was consistent jet formation and the fiber morphology was constant. On the contrary, W50 fibers (0.5 ± 0.14 µm) had smaller diameters but their average was more dispersed as a result of high water content that led to greater viscosity and higher surface tension. A50 fibers (0.56 ± 0.1 µm) had improved uniformity as compared to W50 which was due to the enhanced miscibility of acetic acid and HFIP which resulted in a consistently stable jet formation rate enabling quality fiber formation.

FIGURE 6.1: SEM images and average fiber diameters of electrospun nanofibers prepared using different solvent compositions. a. Control fibers prepared using pure HFIP as the solvent, b. fibers prepared with HFIP + 50% water (W50), and c. fibers prepared with HFIP + 50% acetic acid (A50). Scale bar: 40 µm. **This section is under embargo. The image has been removed and will be made available after the related article is published.**

FTIR spectra were recorded for PCL/gelatin/diclofenac nanofibers prepared with different solvent compositions (HFIP, A50, and W50) to investigate the chemical interactions and structural differences induced by the solvents (Fig 6.2). The spectra exhibited characteristic peaks corresponding to the functional groups of PCL, gelatin, and diclofenac, allowing comparison across the formulations. The blue spectrum (control) represents nanofibers prepared with pure HFIP as the solvent. Sharp and well-defined peaks were observed, including the ester carbonyl stretching (~1700 cm^{-1}), amide bands (~1600–1500 cm^{-1}), and hydroxyl/amine stretching (~3300 cm^{-1}). These results suggest a

uniform distribution of the polymer and drug with minimal secondary interactions, as expected with HFIP, a strong solvent for both PCL and gelatin. The black spectrum (A50), corresponding to nanofibers prepared with HFIP and 50% acetic acid, showed slight shifts and reduced intensity in the carbonyl stretching region (~1700 cm^{-1}). These changes suggest increased polymer-solvent and drug-solvent interactions, as acetic acid promotes better miscibility with the polymer and drug components. The results indicate a potential reduction in polymer crystallinity due to these interactions. The red spectrum (W50), prepared with HFIP and 50% water, exhibited broader peaks, particularly in the OH/NH stretching region (~3300 cm^{-1}). This broadening reflects enhanced hydrogen bonding interactions due to the hydrophilic nature of water, which interacts strongly with gelatin and the diclofenac molecules. Additionally, slight variations in the carbonyl region suggest changes in the fiber matrix structure caused by water as a co-solvent.

The role of the solvent system is critical for affecting the chemical and structural characteristics of the nanofibers. HFIP by itself is used as a standard in order to obtain the formation of homogeneously sized and shaped fibers. The dispersability of the drug within the polymer matrix is also reported to have been improved in A50 which should allow for reduced drug crystallinity. On the other hand, by adding 50% water (W50) creates a hydrogen bonds which may compromise the structural characteristics of the fibers and modify the drug loading and its release. This is also consistent with the drug release profiles that were obtained. These findings show that, indeed, the nanofiber properties can be modulated by the solvent used for their preparation and be tailored for certain medical purposes.

FIGURE 6.2: FTIR spectra of PCL/gelatin/diclofenac nanofibers prepared using different solvent compositions. The blue spectrum represents nanofibers prepared with pure HFIP (ctr), the black spectrum corresponds to nanofibers prepared with 50% acetic acid in HFIP (A50), and the red spectrum represents nanofibers prepared with 50% water in HFIP (W50). **This section is under embargo. The image has been removed and will be made available after the related article is published.**

The release rates of DicNa from PCL/gelatin nanofibers formed with different solvents were evaluated so as to examine their drug delivery capability. Four formulations being A25, A50, W25, and W50 were prepared in which every solution has different amount of acetic acid (A) or water (W) that was added together with HFIP. In this case, A25 and A50 have 25% and 50 % volume of acetic acid with HFIP whereas W25 and W50 have 25 % and 50 % volume of water with HFIP respectively.

FIGURE 6.3: Cumulative DicNa release (%) over time for A25, A50, W25, and W50 formulations. **This section is under embargo. The image has been removed and will be made available after the related article is published.**

Based on the study results (Fig 6.3), a biphasic drug release profile was observed in all formulations. During the first 25 hours, approximately 50-60% of the total drug release was achieved which is associated with a rapid release of the encapsulated diclofenac. This burst phase is assigned to the dissolution of "loosely" adsorbed diclofenac molecules on the surface of nanofibers. After the burst release, a more prolonged, controlled release phase was established, which lasted 175 hours or more. By this time point over 90-100% and approximately the same cumulative release had been attained in all formulations. This repose is explicated in terms of the diffusion control together with the degradation of PCL/gelatin fibers.

The main variables in this study are the solvent composition of the formulations and their release profiles. It has been established that formulations with an addition of acetic acid (A25 and A50) self-release more rapidly than their water counterparts. This is the most likely due to the better miscibility of acetic acid with HFIP which would provide for even dispersion of diclofenac in the fibers matrix making diffusion less restricted. Water-based

formulations (W25 and W50) demonstrated slower release kinetics, particularly W50. This is most likely due to the water based solutions being more hydrophilic, thus having more polymer-drug interactions leading to a lengthy release profile.

The above results show the importance of the solvent used in the formulation and how it can affect the release behaviour of the drug loaded nanofibers. From the above it can be deduced that formulations with acetic acid are likely to provide a faster release which is what is most requiring immediate therapeutic effects, in contrast to water based formulations which offer a slow and controlled release, more for when a sustained delivery of medication is ideal. This study showed the versatility of PCL/gelatin nanofibers in enabling the modification of drug release mechanisms to fit therapeutic requirements.

6.1.3. CONCLUSION

This research showed the adaptability of PCL/gelatin nanofibers drug delivery systems in which the composition of the solvent used for electrospinning had a substantial effect on the release profiles of DicNa. Ionic compounds containing acetic acid (formulations A25 and A50) resulted in a better availability of drugs and faster release, thus could be utilized where immediate effects are needed. In contrast, formulations prepared with water (W25 and W50) could achieve a slower and continuous release rate and could be useful for longterm treatment. These results reveal the versatility of PCL/gelatin nanofibers for a range of biomedical applications such as an immediate dose release or a targeted controlled dose release depending on the type of application required.

6.2. DRUG LOADED MICROGELS

Until now, the primary emphasis of this thesis has been on the electro-spinning type of the EFDTs when creating the nanofibrous drug delivery systems. It is well, however, that electro-spinning has the capacity to fabricate fibrous scaffold with high surface area and controlled drug release kinetics, another universal method offered by EFDT is electrospraying.

In this part, the electrospraying mode of EFDT is investigated for the development of drug loaded microgels. Unlike electrospinning, which forms continuous fibers, electrospraying enables the creation of micro-scale particles with tailored morphology and structure. Such microgels are particularly useful in the encapsulation of bioactive substances due to the ease of controlling encapsulation efficiency and release profiles of these substances.

By electrospraying, it is possible to fabricate microgels with core-shell structure, which can provide biphasic or sustained drug release. The technique, moreover, enables the incorporation of diverse materials, making it suitable for a wide range of biomedical applications. This section will focus on the materials, methods, and outcomes associated with electro-sprayed microgels, highlighting their potential as advanced drug delivery systems.

6.2.1. Materials and Methods

6.2.1.1. Preparation of Alginate Microparticles

Low-viscosity (LV, 250 cPs) and high-viscosity (HV, 20,000–40,000 cPs) sodium alginate (SA) solutions were prepared at 0.5% and 2% w/v, respectively, in deionized water. Core-shell microgels were fabricated using a commercial EFDA system (NF500 MECC, Japan) with a coaxial needle (inner: 27 G, outer: 18 G). Solutions were fed at 0.5 and 2.0 mL/h, under 25 kV voltage and a 150 mm tip-to-collector distance. Droplets were collected in a 1.1% $CaCl_2$ solution to induce ionotropic gelation.

6.2.1.2. Microparticle Characterization

Microparticle morphology was assessed via optical microscopy, and dimensions were analyzed using ImageJ software. FITC-albumin was added to the LV-SA solution for confocal imaging of core-shell architecture. Circularity (CC) was calculated using the equation $C=4\pi(A/P2)C=4\pi(A/P2)$, with $C=1C=1$ indicating a perfect sphere. Alizarin red staining further highlighted core-shell differentiation.

6.2.1.3. Rheological Measurements

Rheological properties of HV and LV alginate solutions were measured at 25°C using a rheometer (Anton Paar MCR 301). Flow curves, strain sweeps, and frequency sweeps were performed to determine shear and viscoelastic behaviors.

6.2.1.4. MATHEMATICAL MODELING

A radial diffusion model was developed in MATLAB to simulate drug release from core-shell microparticles, considering distinct core and shell diffusivities. Simulations were run for a 12-hour release period.

6.2.2. RESULTS AND DISCUSSIONS

The viscosity (η) and viscoelastic properties of polymer solutions play a pivotal role in EFDTs, significantly influencing microparticle morphology. High-viscosity solutions tend to produce larger and spherical microparticles, while low-viscosity solutions yield smaller particles. Rheological characterization revealed Newtonian flow behavior for both Hv and Lv alginate solutions, with average η values of 10^{-1} and 10^{-2} Pa·s, respectively (Figure 6.4a). Normalizing viscosity values using η_0 yielded overlapping master curves (Figure 6.4.b). Oscillatory measurements further showed that the loss modulus (G″) dominated the storage modulus (G′) across the frequency range (Figure 6.4.c).

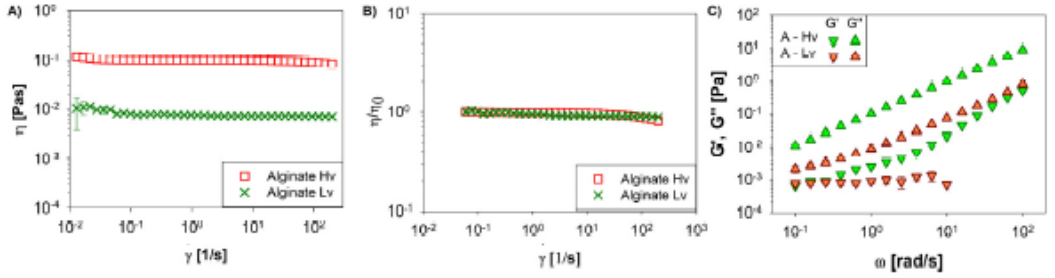

FIGURE 6.4: Rheological properties of sodium alginate solutions with Lv (≈250 cPs) and Hv (20,000–40,000 cPs). a) Viscosity curve versus shear rate. b) Viscosity normalized with respect to the plateau value and b) oscillatory measurements for evaluating G′ and G″.

The morphological and structural properties of core-shell microparticles (CSMp) were analyzed. Utilizing a coaxial needle setup, Lv alginate (≈ 250 cPs) formed the core, while Hv alginate (20,000–40,000 cPs) constituted the shell. Optical microscopy showed smooth, spherical particles with an average diameter of 865.7 ± 28.13 µm, and no agglomeration was observed (Figure 6.5a). The core-shell structure was visualized using Fluorescein Isothiocyanate (FTIC)-albumin labeling, though background noise affected data reproducibility (Figure 6.5b,c). Image analysis recorded an average core diameter of 457.1 ± 63.07 µm, a shell thickness of 254.7 ± 14.25 µm, and a near-perfect circularity of 0.976 ± 0.008. However, the core exhibited slight ovalization (circularity: 0.822 ± 0.058) due to viscosity differences at the core-shell interface.

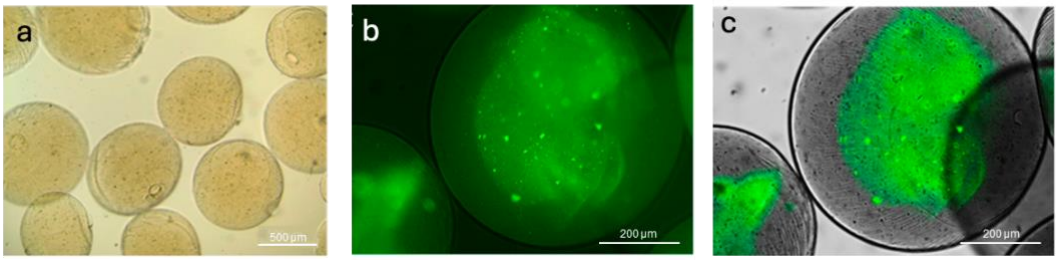

FIGURE 6.5: Sodium alginate microgels with core-shell architecture. a) morphological aspect of microgels via optical microscopy (scale bar: 500 µm), and fluorescence images of microgels with FTIC-albumin-labeled (green) inner phase before b) and after c) image elaboration to remove the background (scale bar: 200 µm).

To further distinguish Hv and Lv phases, alizarin red dye—reactive with Ca^{2+} crosslinkers—was employed (Figure 6.6a). The shell displayed darker staining, indicating a higher concentration of crosslinked calcium ions, while the core exhibited lighter staining due to reduced calcium accessibility. Post-washing, these distinctions were maintained but mitigated by water diffusion (Figure 6.6b).

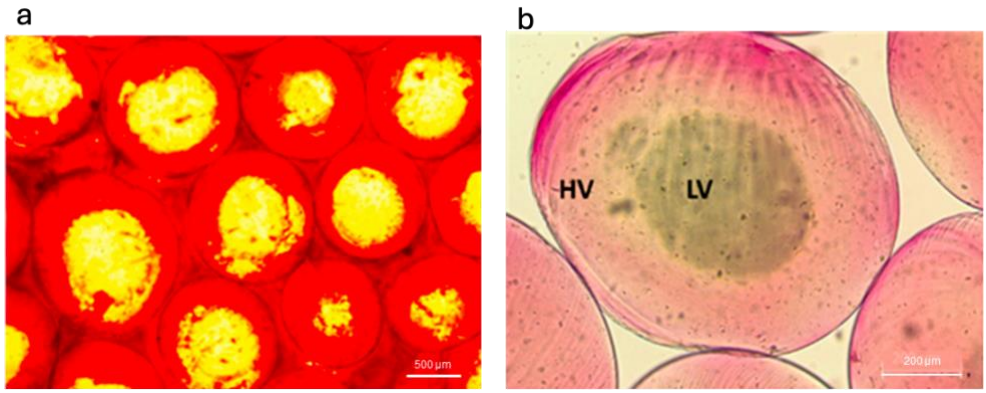

FIGURE 6.6: Dye adsorption: a) Alginate microgels in contact with alizarin red dye (1% in dH_2O) (scale bar: 500 µm) and b) Details of core-shell microgels after washing to remove the excess dye (scale bar: 200 µm).

These alginate microgels demonstrated potential for biomedical applications, including cell interaction support. Previous studies highlight their biocompatibility and ability to maintain mesenchymal stem cell viability. Incorporating bioactive signals or drugs within alginate microparticles can further enhance biological responses, driven by the interplay between chemical composition and structural properties.

A mathematical model was developed to simulate the release of sodium diclofenac through a double-layered alginate hydrogel system. The model assumes isotropic diffusion and radial symmetry, dividing the system into three zones: the inner core (radius R1R1), the shell (radius R2R2), and the external medium (radius R3=10R2R3=10R2). Each zone is characterized by specific diffusivity (DD) and initial concentration values.

Simulations showed that increasing the shell thickness slows the release, reducing the peak height and delaying the maximum flux (R2 value of 1000 µm, there is a tmax ≈ 30 min; for R2 of 1500 µm, there is a tmax ≈ 50 min, and for R2 of 2500 µm, there is a tmax ≈ 100 min). Adjusting the diffusivity ratio between core and shell influences peak height and diffusion rate but not the time of maximum release. These findings highlight the potential to tailor drug-release profiles by modifying shell thickness and diffusivity ratios.

The proposed approach, while demonstrated for sodium diclofenac, can be adapted to other molecules, making alginate a versatile material for designing targeted and sustained drug delivery systems.

6.2.3. CONCLUSIONS

This study highlights the adaptability of electrospraying, an EFDTs, in the production of core-shell alginate microgels as advanced drug delivery systems. According to the rheological characterization determination, the microparticle morphology depends on a solution's viscosity, whereby spherical, larger particles are formed from solutions that have higher viscosity. Core-shell microgels demonstrated a smooth surface, well-defined sizes, as well as structural integrity with proper imaging techniques, core-shell distinction was clearly without confusion due to staining and confocal imaging.

A mathematical diffusion model helped demonstrate the possibility of customizing drug-release kinetics curves by varying shell thickness and diffusivity ratios, thus enabling the postponement of release as well as controlling the amount of flux. All these indicate the possibility of the sustained targeted drug delivery using alginate microgels with the potential for straightforward modification to cater for other bioactive molecules and therapeutic purposes.

Chapter 7

7. CONCLUSION

This thesis describes the novel approach of employing EFDTs in the creating and manufacturing of polymeric composites with applications in tissue engineering, drug delivery and biosensing among others. The research also shows how these techniques can be used to engineer nanofibers and microgels for specific biomedical uses by optimizing-processes such as electrospinning and electrospraying. Some of the paramount achievements include the fabrication of PVA-based nanofibers, scaffolds systems of PVA/gelatin composite for engineering neural tissues and nanofibers with an electroactive matrix of MXene, all of which have the necessary characteristics of advanced biomaterials such as biocompatibility, and the needed mechanical integrity, and also functional performance.

This study establishes a platform for the eco-friendly and reproducible production of functionalized biomaterials, including the water electrospinning and green crosslinking techniques. These developments respond to the needs for environmentally sound options in the biomedical manufacturing sector. The proven capacity to modify the physical attributes of the synthetic biomaterials from the fiber structure to even the electrical properties presents new possibilities in regenerative medicine, controlled release technologies, and bioelectronic devices.

Future research should aim at broader clinical applications of materials manufactured by EFDT. This includes assessing the possibility of scaling up these processes for mass production, and dealing with regulatory issues related to biotechnology. Furthermore, the incorporation of bioactive fillers, growth factors or polymers with ability to respond to external stimuli may increase the functionality of these platforms. Understanding the role

of electrical signals in regulating cellular responses may provide additional opportunities for neural repair and muscle regeneration.

This work justifies EFDT technology as a sophisticated and convenient approach in a field of interest in biomedical engineering that has the potential to develop next-generation biomaterials for applications in personalized medicine, targeted therapy, and many more. This thesis establishes EFDT as a versatile and impactful tool in biomedical engineering, with the potential to shape next-generation biomaterials for personalized medicine.

BIBLIOGRAPHY

[1] Z. Dai and S. Huang, "Functional Dynamics Inside Nano- or Microscale Bio-Hybrid Systems," *Front Chem*, vol. 6, Dec. 2018, doi: 10.3389/fchem.2018.00621.

[2] F. Tian *et al.*, "Quantitative analysis of cell adhesion on aligned micro- and nanofibers," *J Biomed Mater Res A*, vol. 84A, no. 2, pp. 291–299, Feb. 2008, doi: 10.1002/jbm.a.31304.

[3] K. Yoon, B. S. Hsiao, and B. Chu, "Functional nanofibers for environmental applications," *J Mater Chem*, vol. 18, no. 44, p. 5326, 2008, doi: 10.1039/b804128h.

[4] H. N. Kim *et al.*, "Nanotopography-guided tissue engineering and regenerative medicine," *Adv Drug Deliv Rev*, vol. 65, no. 4, pp. 536–558, Apr. 2013, doi: 10.1016/j.addr.2012.07.014.

[5] V. Guarino and L. Ambrosio, "Electrofluidodynamics: Exploring a New Toolbox to Design Biomaterials for Tissue Regeneration and Degeneration," *Nanomedicine*, vol. 11, no. 12, pp. 1515–1518, Jun. 2016, doi: 10.2217/nnm-2016-0108.

[6] S. Haider and A. Haider, Eds., *Electrospinning and Electrospraying - Techniques and Applications*. IntechOpen, 2019. doi: 10.5772/intechopen.77414.

[7] N. Z. Renkler, I. Cruz-Maya, I. Bonadies, and V. Guarino, "Electro Fluid Dynamics: A Route to Design Polymers and Composites for Biomedical and Bio-Sustainable Applications," *Polymers (Basel)*, vol. 14, no. 19, p. 4249, Oct. 2022, doi: 10.3390/polym14194249.

[8] N. Z. Renkler *et al.*, "Micro- and Nanostructured Fibrous Composites via Electro-Fluid Dynamics: Design and Applications for Brain," *Pharmaceutics*, vol. 16, no. 1, p. 134, Jan. 2024, doi: 10.3390/pharmaceutics16010134.

[9] Z. Renkler, I. Cruz Maya, and V. Guarino, "Optimization of Polyvinyl Alcohol-Based Electrospun Fibers with Bioactive or Electroconductive Phases for Tissue-Engineered Scaffolds," *Fibers*, vol. 11, no. 10, p. 85, Oct. 2023, doi: 10.3390/fib11100085.

[10] N. Z. Renkler *et al.*, "Optimizing Electrospun PVA Fibers with MXene Integration as biointerfaces for biosensing applications," *Macromol Mater Eng*, 2025, doi: 10.1002/mame.202400433.

[11] I. Cruz-Maya, C. Schiavone, R. Ferraro, N. Z. Renkler, S. Caserta, and V. Guarino, "Designing Advanced Drug Delivery Systems: Core-Shell Alginate Particles through Electro-Fluid Dynamic Atomization," *Pharmaceutics*, vol. 16, no. 2, Feb. 2024, doi: 10.3390/pharmaceutics16020193.

[12] K. Iranshahi, T. Defraeye, R. M. Rossi, and U. C. Müller, "Electrohydrodynamics and its applications: Recent advances and future perspectives," *Int J Heat Mass Transf*, vol. 232, p. 125895, Nov. 2024, doi: 10.1016/j.ijheatmasstransfer.2024.125895.

[13] V. Guarino, V. Cirillo, R. Altobelli, and L. Ambrosio, "Polymer-based platforms by electric field-assisted techniques for tissue engineering and cancer therapy," *Expert Rev Med Devices*, vol. 12, no. 1, pp. 113–129, Jan. 2015, doi: 10.1586/17434440.2014.953058.

[14] A. Aggarwal and M. K. Sah, "Electrospun materials as scaffolds in tissue engineering and regenerative medicine," in *Biomedical Applications of Electrospinning and Electrospraying*, Elsevier, 2021, pp. 83–121. doi: 10.1016/B978-0-12-822476-2.00005-4.

[15] A. Rahmani Del Bakhshayesh, S. Babaie, B. Niknafs, A. Abedelahi, A. Mehdipour, and M. Ghahremani-Nasab, "High efficiency biomimetic electrospun fibers for use in regenerative medicine and drug delivery: A review," *Mater Chem Phys*, vol. 279, p. 125785, Mar. 2022, doi: 10.1016/j.matchemphys.2022.125785.

[16] K. Valachová, M. A. El Meligy, and L. Šoltés, "Hyaluronic acid and chitosan-based electrospun wound dressings: Problems and solutions," *Int J Biol Macromol*, vol. 206, pp. 74–91, May 2022, doi: 10.1016/j.ijbiomac.2022.02.117.

[17] S. Majumder, M. M. H. Sagor, and M. T. Arafat, "Functional electrospun polymeric materials for bioelectronic devices: a review," *Mater Adv*, vol. 3, no. 17, pp. 6753–6772, 2022, doi: 10.1039/D1MA01114F.

[18] Y. Deng, T. Lu, J. Cui, S. Keshari Samal, R. Xiong, and C. Huang, "Bio-based electrospun nanofiber as building blocks for a novel eco-friendly air filtration membrane: A review," *Sep Purif Technol*, vol. 277, p. 119623, Dec. 2021, doi: 10.1016/j.seppur.2021.119623.

[19] L. Persano, A. Camposeo, C. Tekmen, and D. Pisignano, "Industrial Upscaling of Electrospinning and Applications of Polymer Nanofibers: A Review," *Macromol Mater Eng*, vol. 298, no. 5, pp. 504–520, May 2013, doi: 10.1002/mame.201200290.

[20] I. C. H. H. T. Guideline, "Impurities: Guideline for residual solvents Q3C (R5)," *Current Step*, vol. 4, pp. 1–25, 2005.

[21] S. L. Shenoy, W. D. Bates, H. L. Frisch, and G. E. Wnek, "Role of chain entanglements on fiber formation during electrospinning of polymer solutions: good solvent, non-specific polymer–polymer interaction limit," *Polymer (Guildf)*, vol. 46, no. 10, pp. 3372–3384, Apr. 2005, doi: 10.1016/j.polymer.2005.03.011.

[22] A. G. Şener, A. S. Altay, and F. Altay, "Effect of voltage on morphology of electrospun nanofibers," in *2011 7th International Conference on Electrical and Electronics Engineering (ELECO)*, IEEE, 2011, pp. I–324.

[23] I. Alghoraibi and S. Alomari, "Different Methods for Nanofiber Design and Fabrication," in *Handbook of Nanofibers*, Cham: Springer International Publishing, 2019, pp. 79–124. doi: 10.1007/978-3-319-53655-2_11.

[24] H. Gade, S. Nikam, G. G. Chase, and D. H. Reneker, "Effect of electrospinning conditions on β-phase and surface charge potential of PVDF fibers," *Polymer (Guildf)*, vol. 228, p. 123902, Jul. 2021, doi: 10.1016/j.polymer.2021.123902.

[25] D. Clavijo-Grimaldo, C. A. Casadiego-Torrado, J. Villalobos-Elías, A. Ocampo-Páramo, and M. Torres-Parada, "Characterization of Electrospun Poly(ε-caprolactone) Nano/Micro Fibrous Membrane as Scaffolds in Tissue Engineering: Effects of the Type of Collector Used," *Membranes (Basel)*, vol. 12, no. 6, p. 563, May 2022, doi: 10.3390/membranes12060563.

[26] Y. Ibrahim, E. Hussein, M. Zagho, G. Abdo, and A. Elzatahry, "Melt Electrospinning Designs for Nanofiber Fabrication for Different Applications," *Int J Mol Sci*, vol. 20, no. 10, p. 2455, May 2019, doi: 10.3390/ijms20102455.

[27] G. Yan *et al.*, "Improving Nanofiber Production and Application Performance by Electrospinning at Elevated Temperatures," *Ind Eng Chem Res*, vol. 56, no. 43, pp. 12337–12343, Nov. 2017, doi: 10.1021/acs.iecr.7b02850.

[28] Y.-Z. Long, X. Yan, X.-X. Wang, J. Zhang, and M. Yu, "Electrospinning," in *Electrospinning: Nanofabrication and Applications*, Elsevier, 2019, pp. 21–52. doi: 10.1016/B978-0-323-51270-1.00002-9.

[29] H. Liu, C. R. Gough, Q. Deng, Z. Gu, F. Wang, and X. Hu, "Recent Advances in Electrospun Sustainable Composites for Biomedical, Environmental, Energy, and Packaging Applications," *Int J Mol Sci*, vol. 21, no. 11, p. 4019, Jun. 2020, doi: 10.3390/ijms21114019.

[30] J. Yang, "Biomedical Applications and Research Progress of Electrospinning Technology and Electrospinning Nanofibers," Jan. 19, 2022. doi: 10.14293/S2199-1006.1.SOR-.PPOFGWR.v1.

[31] R. Zhao, X. Lu, and C. Wang, "Electrospinning based all-nano composite materials: Recent achievements and perspectives," *Composites Communications*, vol. 10, pp. 140–150, Dec. 2018, doi: 10.1016/j.coco.2018.09.005.

[32] L. Muthukrishnan, "An overview on electrospinning and its advancement toward hard and soft tissue engineering applications," *Colloid Polym Sci*, vol. 300, no. 8, pp. 875–901, Aug. 2022, doi: 10.1007/s00396-022-04997-9.

[33] A. Pakolpakçıl and Z. Draczynski, "Green Approach to Develop Bee Pollen-Loaded Alginate Based Nanofibrous Mat," *Materials*, vol. 14, no. 11, p. 2775, May 2021, doi: 10.3390/ma14112775.

[34] A. Jaworek and A. T. Sobczyk, "Electrospraying route to nanotechnology: An overview," *J Electrostat*, vol. 66, no. 3–4, pp. 197–219, Mar. 2008, doi: 10.1016/j.elstat.2007.10.001.

[35] R. Sridhar, R. Lakshminarayanan, K. Madhaiyan, V. Amutha Barathi, K. H. C. Lim, and S. Ramakrishna, "Electrosprayed nanoparticles and electrospun nanofibers based on natural materials: applications in tissue regeneration, drug delivery and pharmaceuticals," *Chem Soc Rev*, vol. 44, no. 3, pp. 790–814, 2015, doi: 10.1039/C4CS00226A.

[36] J. Xie, J. Jiang, P. Davoodi, M. P. Srinivasan, and C.-H. Wang, "Electrohydrodynamic atomization: A two-decade effort to produce and process micro-/nanoparticulate materials," *Chem Eng Sci*, vol. 125, pp. 32–57, Mar. 2015, doi: 10.1016/j.ces.2014.08.061.

[37] A. Jaworek, "Micro- and nanoparticle production by electrospraying," *Powder Technol*, vol. 176, no. 1, pp. 18–35, Jul. 2007, doi: 10.1016/j.powtec.2007.01.035.

[38] D. N. Nguyen, C. Clasen, and G. Van den Mooter, "Pharmaceutical Applications of Electrospraying," *J Pharm Sci*, vol. 105, no. 9, pp. 2601–2620, Sep. 2016, doi: 10.1016/j.xphs.2016.04.024.

[39] N. Bock, M. A. Woodruff, D. W. Hutmacher, and T. R. Dargaville, "Electrospraying, a Reproducible Method for Production of Polymeric Microspheres for Biomedical Applications," *Polymers (Basel)*, vol. 3, no. 1, pp. 131–149, Jan. 2011, doi: 10.3390/polym3010131.

[40] J. XIE, J. MARIJNISSEN, and C. WANG, "Microparticles developed by electrohydrodynamic atomization for the local delivery of anticancer drug to treat C6 glioma in vitro," *Biomaterials*, vol. 27, no. 17, pp. 3321–3332, Jun. 2006, doi: 10.1016/j.biomaterials.2006.01.034.

[41] S. Zhang *et al.*, "Coaxial Electrospray Formulations for Improving Oral Absorption of a Poorly Water-Soluble Drug," *Mol Pharm*, vol. 8, no. 3, pp. 807–813, Jun. 2011, doi: 10.1021/mp100401d.

[42] M. Enayati, Z. Ahmad, E. Stride, and M. Edirisinghe, "One-step electrohydrodynamic production of drug-loaded micro- and nanoparticles," *J R Soc Interface*, vol. 7, no. 45, pp. 667–675, Apr. 2010, doi: 10.1098/rsif.2009.0348.

[43] S. Agarwal and A. Greiner, "On the way to clean and safe electrospinning—green electrospinning: emulsion and suspension electrospinning," *Polym Adv Technol*, vol. 22, no. 3, pp. 372–378, Mar. 2011, doi: 10.1002/pat.1883.

[44] R. Abdulhussain, A. Adebisi, B. R. Conway, and K. Asare-Addo, "Electrospun nanofibers: Exploring process parameters, polymer selection, and recent applications in pharmaceuticals and drug delivery," *J Drug Deliv Sci Technol*, vol. 90, p. 105156, Dec. 2023, doi: 10.1016/j.jddst.2023.105156.

[45] S. Li, R. Lv, H. Liu, B. Na, H. Zhou, and L. Ge, "Uniform high-molecular-weight polylactide nanofibers electrospun from a solution below its entanglement concentration," *J Appl Polym Sci*, vol. 134, no. 21, Jun. 2017, doi: 10.1002/app.44853.

[46] F. Topuz and T. Uyar, "Electrospinning of Cyclodextrin Nanofibers: The Effect of Process Parameters," *J Nanomater*, vol. 2020, pp. 1–10, Jun. 2020, doi: 10.1155/2020/7529306.

[47] I. Fatimah, T. I. Sari, and D. Anggoro, "Effect of Concentration and Nozzle-Collector Distance on the Morphology of Nanofibers," *Key Eng Mater*, vol. 860, pp. 315–319, Aug. 2020, doi: 10.4028/www.scientific.net/KEM.860.315.

[48] S. Khandavalli *et al.*, "Toward Optimizing Electrospun Nanofiber Fuel Cell Catalyst Layers: Polymer–Particle Interactions and Spinnability," *ACS Appl Polym Mater*, vol. 3, no. 5, pp. 2374–2384, May 2021, doi: 10.1021/acsapm.0c01354.

[49] A. Haider, S. Haider, and I.-K. Kang, "A comprehensive review summarizing the effect of electrospinning parameters and potential applications of nanofibers in biomedical and biotechnology," *Arabian Journal of Chemistry*, vol. 11, no. 8, pp. 1165–1188, Dec. 2018, doi: 10.1016/j.arabjc.2015.11.015.

[50] D. Shah *et al.*, "Nonwoven Electrospun Membranes as Tissue Scaffolds: Practices, Problems, and Future Directions," *Journal of Composites Science*, vol. 7, no. 12, p. 481, Nov. 2023, doi: 10.3390/jcs7120481.

[51] L. Liverani and A. Boccaccini, "Versatile Production of Poly(Epsilon-Caprolactone) Fibers by Electrospinning Using Benign Solvents," *Nanomaterials*, vol. 6, no. 4, p. 75, Apr. 2016, doi: 10.3390/nano6040075.

[52] D.-G. Yu *et al.*, "Green electrospinning for safe food engineering," Jul. 25, 2023. doi: 10.22541/au.169027404.42481458/v1.

[53] S. Ghosh, A. Yadav, P. M. Gurave, and R. K. Srivastava, "Unique Fiber Morphologies from Emulsion Electrospinning—A Case Study of Poly(ε-caprolactone) and Its Applications," *Colloids and Interfaces*, vol. 7, no. 1, p. 19, Feb. 2023, doi: 10.3390/colloids7010019.

[54] Y. Guan, S. Wu, M. Wang, Y. Tian, W. Lai, and Y. Huang, "Numerical analysis of electrohydrodynamic jet printing under constant and step change of electric voltages," *Physics of Fluids*, vol. 34, no. 6, Jun. 2022, doi: 10.1063/5.0094537.

[55] A. V. Subbotin, "Features of the Behavior of a Polymer Solution Jet in Electrospinning," *Polymer Science, Series A*, vol. 63, no. 2, pp. 172–179, Mar. 2021, doi: 10.1134/S0965545X21020127.

[56] K. Liu, Y. Zheng, C. Ge, B. Xin, and X. Dong, "Preparation and Formation Mechanism of Electrospun Porous Beaded Fibers," *AATCC Journal of Research*, vol. 9, no. 3, pp. 134–142, May 2022, doi: 10.1177/24723444221084394.

[57] I. Fatimah, T. I. Sari, and D. Anggoro, "Effect of Concentration and Nozzle-Collector Distance on the Morphology of Nanofibers," *Key Eng Mater*, vol. 860, pp. 315–319, Aug. 2020, doi: 10.4028/www.scientific.net/KEM.860.315.

[58] X. Li, Y. Zheng, X. Mu, B. Xin, and L. Lin, "Jet motion and fiber properties arising from a parallel electric field in melt-electrospinning," *Textile Research Journal*, vol. 91, no. 7–8, pp. 899–910, Apr. 2021, doi: 10.1177/0040517520964199.

[59] R. Abdulhussain, A. Adebisi, B. R. Conway, and K. Asare-Addo, "Electrospun nanofibers: Exploring process parameters, polymer selection, and recent applications in pharmaceuticals and drug delivery," *J Drug Deliv Sci Technol*, vol. 90, p. 105156, Dec. 2023, doi: 10.1016/j.jddst.2023.105156.

[60] S. Kumar and . P., "Pharmaceutical nanotechnology: Applications in drug delivery," *Pharma Innov*, vol. 8, no. 4, pp. 1315–1319, Apr. 2019, doi: 10.22271/tpi.2019.v8.i4t.25514.

[61] M. Alfadhel, "Nanofiber-Based Drug Delivery Systems: A Review on Its Applications, Challenges, and Envisioning Future Perspectives," *Curr Drug Deliv*, vol. 22, Sep. 2024, doi: 10.2174/0115672018325012240902122946.

[62] S. Malik, S. Subramanian, T. Hussain, A. Nazir, and S. Ramakrishna, "Electrosprayed Nanoparticles as Drug Delivery Systems for Biomedical Applications," *Curr Pharm Des*, vol. 28, no. 5, pp. 368–379, Feb. 2022, doi: 10.2174/1381612827666210929114621.

[63] J. N. Amajuoyi, M. O. Ilomuanya, Y. Asantewaa-Osei, C. P. Azubuike, S. O. Adeosun, and C. I. Igwilo, "Development of electrospun keratin/coenzyme Q10/poly vinyl alcohol nanofibrous scaffold containing mupirocin as potential dressing for infected wounds," *Futur J Pharm Sci*, vol. 6, no. 1, p. 25, Dec. 2020, doi: 10.1186/s43094-020-00043-z.

[64] S. C. Kellaway, M. M. Ullrich, and K. Dziemidowicz, "Electrospun drug-loaded scaffolds for nervous system repair," *WIREs Nanomedicine and Nanobiotechnology*, vol. 16, no. 3, May 2024, doi: 10.1002/wnan.1965.

[65] D. L. Puhl, J. L. Funnell, D. W. Nelson, M. K. Gottipati, and R. J. Gilbert, "Electrospun Fiber Scaffolds for Engineering Glial Cell Behavior to Promote Neural Regeneration," *Bioengineering*, vol. 8, no. 1, p. 4, Dec. 2020, doi: 10.3390/bioengineering8010004.

[66] T. Weigel *et al.*, "Flexible tissue-like electrode as a seamless tissue-electronic interface," *BioNanoMaterials*, vol. 18, no. 3–4, Jan. 2017, doi: 10.1515/bnm-2017-0002.

[67] C.-T. Pan *et al.*, "PVDF/AgNP/MXene composites-based near-field electrospun fiber with enhanced piezoelectric performance for self-powered wearable sensors," *Int J Bioprint*, vol. 9, no. 1, p. 647, Nov. 2022, doi: 10.18063/ijb.v9i1.647.

[68] A. M. Al-Dhahebi, S. C. B. Gopinath, and M. S. M. Saheed, "Graphene impregnated electrospun nanofiber sensing materials: a comprehensive overview on bridging laboratory set-up to industry," *Nano Converg*, vol. 7, no. 1, p. 27, Dec. 2020, doi: 10.1186/s40580-020-00237-4.

[69] F. Mohammadi, A. Valipouri, D. Semnani, and F. Alsahebfosoul, "Nanofibrous Tubular Membrane for Blood Hemodialysis," *Appl Biochem Biotechnol*, vol. 186, no. 2, pp. 443–458, Oct. 2018, doi: 10.1007/s12010-018-2744-0.

[70] X. Yu *et al.*, "High performance thin-film nanofibrous composite hemodialysis membranes with efficient middle-molecule uremic toxin removal," *J Memb Sci*, vol. 523, pp. 173–184, Feb. 2017, doi: 10.1016/j.memsci.2016.09.057.

[71] "Bioinspired Nanomaterials for Drug Delivery," 2021, pp. 63–95. doi: 10.21741/9781644901571-3.

[72] S. Agarwal, J. H. Wendorff, and A. Greiner, "Use of electrospinning technique for biomedical applications," *Polymer (Guildf)*, vol. 49, no. 26, pp. 5603–5621, Dec. 2008, doi: 10.1016/j.polymer.2008.09.014.

[73] N. U. Khaliq, D. Chobisa, C. A. Richard, M. R. Swinney, and Y. Yeo, "Engineering Microenvironment of Biodegradable Polyester Systems for Drug Stability and Release Control," *Ther Deliv*, vol. 12, no. 1, pp. 37–54, Jan. 2021, doi: 10.4155/tde-2020-0113.

[74] N. Z. Renkler, E. Ergene, S. Gokyer, M. Tuzlakoglu Ozturk, P. Yilgor Huri, and K. Tuzlakoglu, "Facile modification of polycaprolactone nanofibers with egg white protein," *J Mater Sci Mater Med*, vol. 32, no. 4, p. 34, Apr. 2021, doi: 10.1007/s10856-021-06505-x.

[75] M. Keshvardoostchokami, S. S. Majidi, P. Huo, R. Ramachandran, M. Chen, and B. Liu, "Electrospun Nanofibers of Natural and Synthetic Polymers as Artificial Extracellular Matrix for Tissue Engineering," *Nanomaterials*, vol. 11, no. 1, p. 21, Dec. 2020, doi: 10.3390/nano11010021.

[76] Z. Terzopoulou, A. Zamboulis, I. Koumentakou, G. Michailidou, M. J. Noordam, and D. N. Bikiaris, "Biocompatible Synthetic Polymers for Tissue Engineering Purposes," *Biomacromolecules*, vol. 23, no. 5, pp. 1841–1863, May 2022, doi: 10.1021/acs.biomac.2c00047.

[77] D. Feldman, "Poly(Vinyl Alcohol) Recent Contributions to Engineering and Medicine," *Journal of Composites Science*, vol. 4, no. 4, p. 175, Nov. 2020, doi: 10.3390/jcs4040175.

[78] G. C. Türkoğlu, N. Khomarloo, E. Mohsenzadeh, D. N. Gospodinova, M. Neznakomova, and F. Salaün, "PVA-Based Electrospun Materials—A Promising Route to Designing Nanofiber Mats with Desired Morphological Shape—A Review," *Int J Mol Sci*, vol. 25, no. 3, p. 1668, Jan. 2024, doi: 10.3390/ijms25031668.

[79] A. S. Elgharbawy, A.-G. M. El Demerdash, W. A. Sadik, M. A. Kasaby, A. H. Lotfy, and A. I. Osman, "Enhancing the Biodegradability, Water Solubility, and Thermal Properties of Polyvinyl Alcohol through Natural Polymer Blending: An Approach toward Sustainable Polymer Applications," *Polymers (Basel)*, vol. 16, no. 15, p. 2141, Jul. 2024, doi: 10.3390/polym16152141.

[80] S. G. Jin, "Production and Application of Biomaterials Based on Polyvinyl alcohol (PVA) as Wound Dressing," *Chem Asian J*, vol. 17, no. 21, Nov. 2022, doi: 10.1002/asia.202200595.

[81] R. M. A. Domingues, S. Chiera, P. Gershovich, A. Motta, R. L. Reis, and M. E. Gomes, "Enhancing the Biomechanical Performance of Anisotropic Nanofibrous Scaffolds in Tendon Tissue Engineering: Reinforcement with Cellulose Nanocrystals," *Adv Healthc Mater*, vol. 5, no. 11, pp. 1364–1375, Jun. 2016, doi: 10.1002/adhm.201501048.

[82] Y. Sánchez-Cardona, C. E. Echeverri-Cuartas, M. E. L. López, and N. Moreno-Castellanos, "Chitosan/Gelatin/PVA Scaffolds for Beta Pancreatic Cell Culture," *Polymers (Basel)*, vol. 13, no. 14, p. 2372, Jul. 2021, doi: 10.3390/polym13142372.

[83] L. Yu, K. Dean, and L. Li, "Polymer blends and composites from renewable resources," *Prog Polym Sci*, vol. 31, no. 6, pp. 576–602, Jun. 2006, doi: 10.1016/j.progpolymsci.2006.03.002.

[84] L. Papadimitriou, P. Manganas, A. Ranella, and E. Stratakis, "Biofabrication for neural tissue engineering applications," *Mater Today Bio*, vol. 6, p. 100043, Mar. 2020, doi: 10.1016/j.mtbio.2020.100043.

[85] W. Guo *et al.*, "Construction of a 3D rGO–collagen hybrid scaffold for enhancement of the neural differentiation of mesenchymal stem cells," *Nanoscale*, vol. 8, no. 4, pp. 1897–1904, 2016, doi: 10.1039/C5NR06602F.

[86] L. S. Pires, F. D. Magalhães, and A. M. Pinto, "New Polymeric Composites Based on Two-Dimensional Nanomaterials for Biomedical Applications," *Polymers (Basel)*, vol. 14, no. 7, p. 1464, Apr. 2022, doi: 10.3390/polym14071464.

[87] A. Rybak, "Functional Polymer Composite with Core-Shell Ceramic Filler: II. Rheology, Thermal, Mechanical, and Dielectric Properties," *Polymers (Basel)*, vol. 13, no. 13, p. 2161, Jun. 2021, doi: 10.3390/polym13132161.

[88] I. F. Wahab, S. I. A. Razak, N. S. Azmi, F. N. Dahli, A. H. M. Yusof, and N. H. M. Nayan, "Electrospun Graphene Oxide-Based Nanofibres," in *Advances in Carbon Nanostructures*, InTech, 2016. doi: 10.5772/64055.

[89] S. M. Majhi, A. Mirzaei, H. W. Kim, and S. S. Kim, "Reduced Graphene Oxide (rGO)-Loaded Metal-Oxide Nanofiber Gas Sensors: An Overview," *Sensors*, vol. 21, no. 4, p. 1352, Feb. 2021, doi: 10.3390/s21041352.

[90] Y. S. Koo *et al.*, "Enhancement of Electrical Conductivity of Electrospun Polyacrylonitrile Fibres Using Carbon Nanomaterials Synthesised from

Polypropylene Waste," *Materials Science Forum*, vol. 1010, pp. 111–117, Sep. 2020, doi: 10.4028/www.scientific.net/MSF.1010.111.

[91] K. Belabbes *et al.*, "Development of hybrid bioactive nanofibers composed of star Poly(lactic acid) and gelatin by sol–gel crosslinking during the electrospinning process," *Nanotechnology*, vol. 34, no. 48, p. 485701, Nov. 2023, doi: 10.1088/1361-6528/acf501.

[92] R. Wu, H. Li, Y. Yang, Q. Zheng, S. Li, and Y. Chen, "Bioactive Silk Fibroin-Based Hybrid Biomaterials for Musculoskeletal Engineering: Recent Progress and Perspectives," *ACS Appl Bio Mater*, vol. 4, no. 9, pp. 6630–6646, Sep. 2021, doi: 10.1021/acsabm.1c00654.

[93] B. Abadi, N. Goshtasbi, S. Bolourian, J. Tahsili, M. Adeli-Sardou, and H. Forootanfar, "Electrospun hybrid nanofibers: Fabrication, characterization, and biomedical applications," *Front Bioeng Biotechnol*, vol. 10, Dec. 2022, doi: 10.3389/fbioe.2022.986975.

[94] T. R. de Lima Nascimento *et al.*, "Current Applications of Biopolymer-based Scaffolds and Nanofibers as Drug Delivery Systems," *Curr Pharm Des*, vol. 25, no. 37, pp. 3997–4012, Dec. 2019, doi: 10.2174/1381612825666191108162948.

[95] G. Rivera-Hernández, M. Antunes-Ricardo, P. Martínez-Morales, and M. L. Sánchez, "Polyvinyl alcohol based-drug delivery systems for cancer treatment," *Int J Pharm*, vol. 600, p. 120478, May 2021, doi: 10.1016/j.ijpharm.2021.120478.

[96] O. DALYAN, Ö. F. ÖZTÜRK, and M. PİŞKİN, "Toxicity of polyvinyl alcohols in medicinal chemistry," *MANAS Journal of Engineering*, vol. 9, no. 2, pp. 129–135, Dec. 2021, doi: 10.51354/mjen.918635.

[97] S. Waheed, A. L. Butcher, and M. L. Oyen, "The viscoelastic response of electrospun poly(vinyl alcohol) mats," *J Mech Behav Biomed Mater*, vol. 77, pp. 383–388, Jan. 2018, doi: 10.1016/j.jmbbm.2017.09.029.

[98] M. S. Peresin, Y. Habibi, J. O. Zoppe, J. J. Pawlak, and O. J. Rojas, "Nanofiber Composites of Polyvinyl Alcohol and Cellulose Nanocrystals: Manufacture and Characterization," *Biomacromolecules*, vol. 11, no. 3, pp. 674–681, Mar. 2010, doi: 10.1021/bm901254n.

[99] P. Moradipour, M. Limoee, S. Janfaza, and L. Behbood, "Core-Shell Nanofibers Based on Polycaprolactone/Polyvinyl Alcohol and Polycaprolactone/Collagen for Biomedical Applications," *J Pharm Innov*, vol. 17, no. 3, pp. 911–920, Sep. 2022, doi: 10.1007/s12247-021-09568-z.

[100] Y. Mao *et al.*, "Electrospun polymers: Using devices to enhance their potential for biomedical applications," *React Funct Polym*, vol. 186, p. 105568, May 2023, doi: 10.1016/j.reactfunctpolym.2023.105568.

[101] J.-C. Park *et al.*, "Electrospun poly(vinyl alcohol) nanofibers: effects of degree of hydrolysis and enhanced water stability," *Polym J*, vol. 42, no. 3, pp. 273–276, Mar. 2010, doi: 10.1038/pj.2009.340.

[102] A. Al-Abduljabbar and I. Farooq, "Electrospun Polymer Nanofibers: Processing, Properties, and Applications," *Polymers (Basel)*, vol. 15, no. 1, p. 65, Dec. 2022, doi: 10.3390/polym15010065.

[103] T. Baykara and G. Taylan, "Coaxial electrospinning of PVA/Nigella seed oil nanofibers: Processing and morphological characterization," *Materials Science and Engineering: B*, vol. 265, p. 115012, Mar. 2021, doi: 10.1016/j.mseb.2020.115012.

[104] M. Alazab, G. R. Mitchell, F. J. Davis, and S. D. Mohan, "Sustainable Electrospinning of Nanoscale Fibres," *Procedia Manuf*, vol. 12, pp. 66–78, 2017, doi: 10.1016/j.promfg.2017.08.009.

[105] M. U. Aslam Khan *et al.*, "Recent Advances in Biopolymeric Composite Materials for Tissue Engineering and Regenerative Medicines: A Review," *Molecules*, vol. 26, no. 3, p. 619, Jan. 2021, doi: 10.3390/molecules26030619.

[106] E. Rynkowska, K. Fatyeyeva, S. Marais, J. Kujawa, and W. Kujawski, "Chemically and Thermally Crosslinked PVA-Based Membranes: Effect on Swelling and Transport Behavior," *Polymers (Basel)*, vol. 11, no. 11, p. 1799, Nov. 2019, doi: 10.3390/polym11111799.

[107] M. S. Peresin, Y. Habibi, J. O. Zoppe, J. J. Pawlak, and O. J. Rojas, "Nanofiber Composites of Polyvinyl Alcohol and Cellulose Nanocrystals: Manufacture and Characterization," *Biomacromolecules*, vol. 11, no. 3, pp. 674–681, Mar. 2010, doi: 10.1021/bm901254n.

[108] B. Imre and B. Pukánszky, "Compatibilization in bio-based and biodegradable polymer blends," *Eur Polym J*, vol. 49, no. 6, pp. 1215–1233, Jun. 2013, doi: 10.1016/j.eurpolymj.2013.01.019.

[109] S. Mares-Bou, M.-A. Serrano, and J. A. Gómez-Tejedor, "Core–Shell Polyvinyl Alcohol (PVA) Base Electrospinning Microfibers for Drug Delivery," *Polymers (Basel)*, vol. 15, no. 6, p. 1554, Mar. 2023, doi: 10.3390/polym15061554.

[110] K. Vacheethasanee, S. Wang, Y. Qiu, and R. E. Marchant, "Poly(ethylene oxide) surfactant polymers," *J Biomater Sci Polym Ed*, vol. 15, no. 1, pp. 95–110, Jan. 2004, doi: 10.1163/156856204322752255.

[111] H. Liu and B. Zuo, "Structure and Sound Absorption Properties of Spiral Vane Electrospun PVA/PEO Nanofiber Membranes," *Applied Sciences*, vol. 8, no. 2, p. 296, Feb. 2018, doi: 10.3390/app8020296.

[112] M. C. Gómez-Guillén, B. Giménez, M. E. López-Caballero, and M. P. Montero, "Functional and bioactive properties of collagen and gelatin from alternative sources: A review," *Food Hydrocoll*, vol. 25, no. 8, pp. 1813–1827, Dec. 2011, doi: 10.1016/j.foodhyd.2011.02.007.

[113] A. Gaspar-Pintiliescu, A.-M. Stanciuc, and O. Craciunescu, "Natural composite dressings based on collagen, gelatin and plant bioactive compounds for wound

healing: A review," *Int J Biol Macromol*, vol. 138, pp. 854–865, Oct. 2019, doi: 10.1016/j.ijbiomac.2019.07.155.

[114] S. Ferraris *et al.*, "Topographical and Biomechanical Guidance of Electrospun Fibers for Biomedical Applications," *Polymers (Basel)*, vol. 12, no. 12, p. 2896, Dec. 2020, doi: 10.3390/polym12122896.

[115] M. Yousefzadeh, "Modeling and simulation of the electrospinning process," in *Electrospun Nanofibers*, Elsevier, 2017, pp. 277–301. doi: 10.1016/B978-0-08-100907-9.00012-X.

[116] S. K. Sharma, J. Prakash, and P. K. Pujari, "Effects of the molecular level dispersion of graphene oxide on the free volume characteristics of poly(vinyl alcohol) and its impact on the thermal and mechanical properties of their nanocomposites," *Physical Chemistry Chemical Physics*, vol. 17, no. 43, pp. 29201–29209, 2015, doi: 10.1039/C5CP05278E.

[117] Q. Yang *et al.*, "Improved biomedical bioactivity of polyvinyl alcohol/polyethylene oxide composite system-based nanofiber membranes via incorporating Antarctic krill protein," *Eur Polym J*, vol. 187, p. 111888, Apr. 2023, doi: 10.1016/j.eurpolymj.2023.111888.

[118] L. Jia and X. Qin, "The effect of different surfactants on the electrospinning poly(vinyl alcohol) (PVA) nanofibers," *J Therm Anal Calorim*, vol. 112, no. 2, pp. 595–605, May 2013, doi: 10.1007/s10973-012-2607-9.

[119] J.-Y. Zheng *et al.*, "The Effect of Surfactants on the Diameter and Morphology of Electrospun Ultrafine Nanofiber," *J Nanomater*, vol. 2014, no. 1, Jan. 2014, doi: 10.1155/2014/689298.

[120] M. A. Taemeh, A. Shiravandi, M. A. Korayem, and H. Daemi, "Fabrication challenges and trends in biomedical applications of alginate electrospun nanofibers," *Carbohydr Polym*, vol. 228, p. 115419, Jan. 2020, doi: 10.1016/j.carbpol.2019.115419.

[121] J. Avossa, G. Herwig, C. Toncelli, F. Itel, and R. M. Rossi, "Electrospinning based on benign solvents: current definitions, implications and strategies," *Green Chemistry*, vol. 24, no. 6, pp. 2347–2375, 2022, doi: 10.1039/D1GC04252A.

[122] E. Hirsch *et al.*, "Probiotic bacteria stabilized in orally dissolving nanofibers prepared by high-speed electrospinning," *Food and Bioproducts Processing*, vol. 128, pp. 84–94, Jul. 2021, doi: 10.1016/j.fbp.2021.04.016.

[123] W. Shen and Y.-L. Hsieh, "Biocompatible sodium alginate fibers by aqueous processing and physical crosslinking," *Carbohydr Polym*, vol. 102, pp. 893–900, Feb. 2014, doi: 10.1016/j.carbpol.2013.10.066.

[124] R. Salihu *et al.*, "Citric acid: A green cross-linker of biomaterials for biomedical applications," *Eur Polym J*, vol. 146, p. 110271, Mar. 2021, doi: 10.1016/j.eurpolymj.2021.110271.

[125] D. Nataraj, R. Reddy, and N. Reddy, "Crosslinking electrospun poly (vinyl) alcohol fibers with citric acid to impart aqueous stability for medical applications," *Eur Polym J*, vol. 124, p. 109484, Feb. 2020, doi: 10.1016/j.eurpolymj.2020.109484.

[126] Z. Lian and L. Ye, "Structure and properties of PVA/PEO hydrogel prepared by freezing/thawing method," *Journal of Thermoplastic Composite Materials*, vol. 26, no. 7, pp. 912–922, Aug. 2013, doi: 10.1177/0892705711430857.

[127] H. Liu and B. Zuo, "Sound absorption property of PVA/PEO/GO nanofiber membrane and non-woven composite material," *Journal of Industrial Textiles*, vol. 50, no. 4, pp. 512–525, Oct. 2020, doi: 10.1177/1528083719832857.

[128] J. Zhang *et al.*, "Thermally Treated Berberine-Loaded SA/PVA/PEO Electrospun Microfiber Membranes for Antibacterial Wound Dressings," *Polymers (Basel)*, vol. 14, no. 21, p. 4473, Oct. 2022, doi: 10.3390/polym14214473.

[129] D. Yu, Y. Feng, J. Xu, B. Kong, Q. Liu, and H. Wang, "Fabrication, characterization, and antibacterial properties of citric acid crosslinked PVA electrospun microfibre

mats for active food packaging," *Packaging Technology and Science*, vol. 34, no. 6, pp. 361–370, Jun. 2021, doi: 10.1002/pts.2566.

[130] S. G. Pathan *et al.*, "Cytotoxicity associated with electrospun polyvinyl alcohol," *J Biomed Mater Res B Appl Biomater*, vol. 103, no. 8, pp. 1652–1662, Nov. 2015, doi: 10.1002/jbm.b.33337.

[131] H. Lv *et al.*, "Electrospun Chitosan–Polyvinyl Alcohol Nanofiber Dressings Loaded with Bioactive Ursolic Acid Promoting Diabetic Wound Healing," *Nanomaterials*, vol. 12, no. 17, p. 2933, Aug. 2022, doi: 10.3390/nano12172933.

[132] A. Asiri, S. Saidin, M. H. Sani, and R. H. Al-Ashwal, "Epidermal and fibroblast growth factors incorporated polyvinyl alcohol electrospun nanofibers as biological dressing scaffold," *Sci Rep*, vol. 11, no. 1, p. 5634, Mar. 2021, doi: 10.1038/s41598-021-85149-x.

[133] D. O. Sanchez Ramirez, I. Cruz-Maya, C. Vineis, C. Tonetti, A. Varesano, and V. Guarino, "Design of Asymmetric Nanofibers-Membranes Based on Polyvinyl Alcohol and Wool-Keratin for Wound Healing Applications," *J Funct Biomater*, vol. 12, no. 4, p. 76, Dec. 2021, doi: 10.3390/jfb12040076.

[134] M. Koosha and H. Mirzadeh, "Electrospinning, mechanical properties, and cell behavior study of chitosan/ <scp>PVA</scp> nanofibers," *J Biomed Mater Res A*, vol. 103, no. 9, pp. 3081–3093, Sep. 2015, doi: 10.1002/jbm.a.35443.

[135] Y. Deng *et al.*, "Peptide-decorated polyvinyl alcohol/hyaluronan nanofibers for human induced pluripotent stem cell culture," *Carbohydr Polym*, vol. 101, pp. 36–39, Jan. 2014, doi: 10.1016/j.carbpol.2013.09.030.

[136] C. Qiao, X. Ma, J. Zhang, and J. Yao, "Molecular interactions in gelatin/chitosan composite films," *Food Chem*, vol. 235, pp. 45–50, Nov. 2017, doi: 10.1016/j.foodchem.2017.05.045.

[137] N. Davidenko *et al.*, "Evaluation of cell binding to collagen and gelatin: a study of the effect of 2D and 3D architecture and surface chemistry," *J Mater Sci Mater Med*, vol. 27, no. 10, p. 148, Oct. 2016, doi: 10.1007/s10856-016-5763-9.

[138] A. Gaspar-Pintiliescu, A.-M. Stanciuc, and O. Craciunescu, "Natural composite dressings based on collagen, gelatin and plant bioactive compounds for wound healing: A review," *Int J Biol Macromol*, vol. 138, pp. 854–865, Oct. 2019, doi: 10.1016/j.ijbiomac.2019.07.155.

[139] B. Zavan *et al.*, "Electrospun PCL-Based Vascular Grafts: In Vitro Tests," *Nanomaterials*, vol. 11, no. 3, p. 751, Mar. 2021, doi: 10.3390/nano11030751.

[140] M. Uz, M. Donta, M. Mededovic, D. S. Sakaguchi, and S. K. Mallapragada, "Development of Gelatin and Graphene-Based Nerve Regeneration Conduits Using Three-Dimensional (3D) Printing Strategies for Electrical Transdifferentiation of Mesenchymal Stem Cells," *Ind Eng Chem Res*, vol. 58, no. 18, pp. 7421–7427, May 2019, doi: 10.1021/acs.iecr.8b05537.

[141] V. Cirillo, V. Guarino, M. A. Alvarez-Perez, M. Marrese, and L. Ambrosio, "Optimization of fully aligned bioactive electrospun fibers for 'in vitro' nerve guidance," *J Mater Sci Mater Med*, vol. 25, no. 10, pp. 2323–2332, Oct. 2014, doi: 10.1007/s10856-014-5214-4.

[142] W. K. W. Abdul Khodir, A. H. Abdul Razak, M. H. Ng, V. Guarino, and D. Susanti, "Encapsulation and Characterization of Gentamicin Sulfate in the Collagen Added Electrospun Nanofibers for Skin Regeneration," *J Funct Biomater*, vol. 9, no. 2, p. 36, May 2018, doi: 10.3390/jfb9020036.

[143] C. Vineis *et al.*, "Synergistic effect of sericin and keratin in gelatin based nanofibers for in vitro applications," *Int J Biol Macromol*, vol. 190, pp. 375–381, Nov. 2021, doi: 10.1016/j.ijbiomac.2021.09.007.

[144] I. Cruz-Maya, V. Guarino, A. Almaguer-Flores, M. A. Alvarez-Perez, A. Varesano, and C. Vineis, "Highly polydisperse keratin rich nanofibers: Scaffold design and *in*

vitro characterization," *J Biomed Mater Res A*, vol. 107, no. 8, pp. 1803–1813, Aug. 2019, doi: 10.1002/jbm.a.36699.

[145] E. Saracino *et al.*, "Structural and functional properties of astrocytes on PCL based electrospun fibres," *Materials Science and Engineering: C*, vol. 118, p. 111363, Jan. 2021, doi: 10.1016/j.msec.2020.111363.

[146] X. Huang *et al.*, "Astroglial Connexins in Neurodegenerative Diseases," *Front Mol Neurosci*, vol. 14, May 2021, doi: 10.3389/fnmol.2021.657514.

[147] A. V. Molofsky and B. Deneen, "Astrocyte development: A Guide for the Perplexed," *Glia*, vol. 63, no. 8, pp. 1320–1329, Aug. 2015, doi: 10.1002/glia.22836.

[148] Z. Renkler, I. Cruz Maya, and V. Guarino, "Optimization of Polyvinyl Alcohol-Based Electrospun Fibers with Bioactive or Electroconductive Phases for Tissue-Engineered Scaffolds," *Fibers*, vol. 11, no. 10, p. 85, Oct. 2023, doi: 10.3390/fib11100085.

[149] H. Y. Chi *et al.*, "Fabrication of Gelatin Nanofibers by Electrospinning—Mixture of Gelatin and Polyvinyl Alcohol," *Polymers (Basel)*, vol. 14, no. 13, p. 2610, Jun. 2022, doi: 10.3390/polym14132610.

[150] R. Liu, J. Ming, H. Zhang, and B. Zuo, "EDC/NHS crosslinked electrospun regenerated tussah silk fibroin nanofiber mats," *Fibers and Polymers*, vol. 13, no. 5, pp. 613–617, May 2012, doi: 10.1007/s12221-012-0613-y.

[151] G. P. Nicchia *et al.*, "Aquaporin-4-containing astrocytes sustain a temperature- and mercury-insensitive swelling in vitro," *Glia*, vol. 31, no. 1, pp. 29–38, Jul. 2000, doi: 10.1002/(SICI)1098-1136(200007)31:1<29::AID-GLIA30>3.0.CO;2-3.

[152] N. Bhardwaj and S. C. Kundu, "Electrospinning: A fascinating fiber fabrication technique," *Biotechnol Adv*, vol. 28, no. 3, pp. 325–347, May 2010, doi: 10.1016/j.biotechadv.2010.01.004.

[153] J. Ma, L. Zhang, and B. Lei, "Multifunctional MXene-Based Bioactive Materials for Integrated Regeneration Therapy," *ACS Nano*, vol. 17, no. 20, pp. 19526–19549, Oct. 2023, doi: 10.1021/acsnano.3c01913.

[154] X. Mi, Z. Su, Y. Fu, S. Li, and A. Mo, "3D printing of Ti_3C_2 -MXene-incorporated composite scaffolds for accelerated bone regeneration," *Biomedical Materials*, vol. 17, no. 3, p. 035002, May 2022, doi: 10.1088/1748-605X/ac5ffe.

[155] K. Yang *et al.*, "Biodegradable polyvinyl alcohol/nano-hydroxyapatite composite membrane enhanced by MXene nanosheets for guided bone regeneration," *J Mech Behav Biomed Mater*, vol. 155, p. 106540, Jul. 2024, doi: 10.1016/j.jmbbm.2024.106540.

[156] T. Zhou *et al.*, "Ultra-compact MXene fibers by continuous and controllable synergy of interfacial interactions and thermal drawing-induced stresses," *Nat Commun*, vol. 13, no. 1, p. 4564, Aug. 2022, doi: 10.1038/s41467-022-32361-6.

[157] P. Sobolčiak *et al.*, "2D Ti3C2Tx (MXene)-reinforced polyvinyl alcohol (PVA) nanofibers with enhanced mechanical and electrical properties," *PLoS One*, vol. 12, no. 8, p. e0183705, Aug. 2017, doi: 10.1371/journal.pone.0183705.

[158] M. Rafiq *et al.*, "Recent progress in MXenes incorporated into electrospun nanofibers for biomedical application: Study focusing from 2017 to 2022," *Chinese Chemical Letters*, vol. 34, no. 7, p. 108463, Jul. 2023, doi: 10.1016/j.cclet.2023.108463.

[159] K. H. Tan, L. Samylingam, N. Aslfattahi, R. Saidur, and K. Kadirgama, "Optical and conductivity studies of polyvinyl alcohol-MXene (PVA-MXene) nanocomposite thin films for electronic applications," *Opt Laser Technol*, vol. 136, p. 106772, Apr. 2021, doi: 10.1016/j.optlastec.2020.106772.

[160] S. Ling *et al.*, "Facile synthesis of MXene−Polyvinyl alcohol hybrid material for robust flexible memristor," *J Solid State Chem*, vol. 318, p. 123731, Feb. 2023, doi: 10.1016/j.jssc.2022.123731.

[161] J. Dong, Z. Li, C. Liu, B. Zhou, C. Liu, and Y. Feng, "Highly oriented MXene/polyvinyl alcohol films prepared by scalable layer-by-layer blade coating for

efficient electromagnetic interference shielding and infrared stealth," *Nano Res*, vol. 17, no. 6, pp. 5651–5660, Jun. 2024, doi: 10.1007/s12274-024-6486-8.

[162] M. M. Pereira, J. R. Jones, and L. L. Hench, "Bioactive glass and hybrid scaffolds prepared by sol–gel method for bone tissue engineering," *Advances in Applied Ceramics*, vol. 104, no. 1, pp. 35–42, Feb. 2005, doi: 10.1179/174367605225011034.

[163] M. Mahmoudi, P. Alizadeh, and M. Soltani, "Wound healing performance of electrospun PVA/70S30C bioactive glass/Ag nanoparticles mats decorated with curcumin: In vitro and in vivo investigations," *Biomaterials Advances*, vol. 153, p. 213530, Oct. 2023, doi: 10.1016/j.bioadv.2023.213530.

[164] M. Riccio *et al.*, "Current distribution effects in organic sexithiophene field effect transistors investigated by lock-in thermography: Mobility evaluation issues," *Appl Phys Lett*, vol. 93, no. 24, Dec. 2008, doi: 10.1063/1.3049613.

[165] D. L. Puhl, J. L. Funnell, D. W. Nelson, M. K. Gottipati, and R. J. Gilbert, "Electrospun Fiber Scaffolds for Engineering Glial Cell Behavior to Promote Neural Regeneration," *Bioengineering*, vol. 8, no. 1, p. 4, Dec. 2020, doi: 10.3390/bioengineering8010004.

[166] E. A. Mayerberger, O. Urbanek, R. M. McDaniel, R. M. Street, M. W. Barsoum, and C. L. Schauer, "Preparation and characterization of polymer-$Ti_3C_2T_x$ (MXene) composite nanofibers produced via electrospinning," *J Appl Polym Sci*, vol. 134, no. 37, Oct. 2017, doi: 10.1002/app.45295.

[167] H. Zhang, D. Lan, X. Li, Z. Li, and F. Dai, "Conductive and antibacterial scaffold with rapid crimping property for application prospect in repair of peripheral nerve injury," *J Appl Polym Sci*, vol. 140, no. 5, Feb. 2023, doi: 10.1002/app.53426.

[168] G. P. Awasthi *et al.*, "Synthesis, characterizations, and biocompatibility evaluation of polycaprolactone–MXene electrospun fibers," *Colloids Surf A Physicochem Eng Asp*, vol. 586, p. 124282, Feb. 2020, doi: 10.1016/j.colsurfa.2019.124282.

[169] P. Sobolčiak *et al.*, "2D Ti3C2Tx (MXene)-reinforced polyvinyl alcohol (PVA) nanofibers with enhanced mechanical and electrical properties," *PLoS One*, vol. 12, no. 8, p. e0183705, Aug. 2017, doi: 10.1371/journal.pone.0183705.

[170] T. A. Hamdalla, T. A. Hanafy, and A. E. Bekheet, "Influence of Erbium Ions on the Optical and Structural Properties of Polyvinyl Alcohol," *Journal of Spectroscopy*, vol. 2015, pp. 1–7, 2015, doi: 10.1155/2015/204867.

[171] K. Hussain *et al.*, "Terahertz time-domain spectroscopy of thin and flexible CNT-modified MXene/polymer composites," *Applied Physics A*, vol. 127, no. 5, p. 382, May 2021, doi: 10.1007/s00339-021-04525-6.

[172] X. He *et al.*, "A high-performance waterborne polymeric composite coating with long-term anti-corrosive property based on phosphorylation of chitosan-functionalized Ti3C2Tx MXene," *Adv Compos Hybrid Mater*, vol. 5, no. 3, pp. 1699–1711, Sep. 2022, doi: 10.1007/s42114-021-00392-0.

[173] K. H. Tan, L. Samylingam, N. Aslfattahi, R. Saidur, and K. Kadirgama, "Optical and conductivity studies of polyvinyl alcohol-MXene (PVA-MXene) nanocomposite thin films for electronic applications," *Opt Laser Technol*, vol. 136, p. 106772, Apr. 2021, doi: 10.1016/j.optlastec.2020.106772.

[174] M. Riccio *et al.*, "Current distribution effects in organic sexithiophene field effect transistors investigated by lock-in thermography: Mobility evaluation issues," *Appl Phys Lett*, vol. 93, no. 24, Dec. 2008, doi: 10.1063/1.3049613.

[175] A. Rianjanu, A. Kusumaatmaja, E. A. Suyono, and K. Triyana, "Solvent vapor treatment improves mechanical strength of electrospun polyvinyl alcohol nanofibers," *Heliyon*, vol. 4, no. 4, p. e00592, Apr. 2018, doi: 10.1016/j.heliyon.2018.e00592.

[176] N. H. A. Ngadiman, M. Y. Noordin, A. Idris, A. S. A. Shakir, and D. Kurniawan, "Influence of Polyvinyl Alcohol Molecular Weight on the Electrospun Nanofiber

Mechanical Properties," *Procedia Manuf*, vol. 2, pp. 568–572, 2015, doi: 10.1016/j.promfg.2015.07.098.

[177] P. Sobolčiak *et al.*, "2D Ti3C2Tx (MXene)-reinforced polyvinyl alcohol (PVA) nanofibers with enhanced mechanical and electrical properties," *PLoS One*, vol. 12, no. 8, p. e0183705, Aug. 2017, doi: 10.1371/journal.pone.0183705.

[178] A. Rianjanu, A. Kusumaatmaja, E. A. Suyono, and K. Triyana, "Solvent vapor treatment improves mechanical strength of electrospun polyvinyl alcohol nanofibers," *Heliyon*, vol. 4, no. 4, p. e00592, Apr. 2018, doi: 10.1016/j.heliyon.2018.e00592.

[179] J. S. Jeong, J. S. Moon, S. Y. Jeon, J. H. Park, P. S. Alegaonkar, and J. B. Yoo, "Mechanical properties of electrospun PVA/MWNTs composite nanofibers," *Thin Solid Films*, vol. 515, no. 12, pp. 5136–5141, Apr. 2007, doi: 10.1016/j.tsf.2006.10.058.

[180] N. H. A. Ngadiman, M. Y. Noordin, A. Idris, A. S. A. Shakir, and D. Kurniawan, "Influence of Polyvinyl Alcohol Molecular Weight on the Electrospun Nanofiber Mechanical Properties," *Procedia Manuf*, vol. 2, pp. 568–572, 2015, doi: 10.1016/j.promfg.2015.07.098.

[181] P. Sobolčiak *et al.*, "2D Ti3C2Tx (MXene)-reinforced polyvinyl alcohol (PVA) nanofibers with enhanced mechanical and electrical properties," *PLoS One*, vol. 12, no. 8, p. e0183705, Aug. 2017, doi: 10.1371/journal.pone.0183705.

[182] J. S. Jeong, J. S. Moon, S. Y. Jeon, J. H. Park, P. S. Alegaonkar, and J. B. Yoo, "Mechanical properties of electrospun PVA/MWNTs composite nanofibers," *Thin Solid Films*, vol. 515, no. 12, pp. 5136–5141, Apr. 2007, doi: 10.1016/j.tsf.2006.10.058.

[183] M. Koosha and H. Mirzadeh, "Electrospinning, mechanical properties, and cell behavior study of chitosan/ <scp>PVA</scp> nanofibers," *J Biomed Mater Res A*, vol. 103, no. 9, pp. 3081–3093, Sep. 2015, doi: 10.1002/jbm.a.35443.

[184] Z. Renkler, I. Cruz Maya, and V. Guarino, "Optimization of Polyvinyl Alcohol-Based Electrospun Fibers with Bioactive or Electroconductive Phases for Tissue-Engineered Scaffolds," *Fibers*, vol. 11, no. 10, p. 85, Oct. 2023, doi: 10.3390/fib11100085.

[185] S. G. Jin, "Production and Application of Biomaterials Based on Polyvinyl alcohol (PVA) as Wound Dressing," *Chem Asian J*, vol. 17, no. 21, Nov. 2022, doi: 10.1002/asia.202200595.

[186] D. O. Sanchez Ramirez, I. Cruz-Maya, C. Vineis, C. Tonetti, A. Varesano, and V. Guarino, "Design of Asymmetric Nanofibers-Membranes Based on Polyvinyl Alcohol and Wool-Keratin for Wound Healing Applications," *J Funct Biomater*, vol. 12, no. 4, p. 76, Dec. 2021, doi: 10.3390/jfb12040076.

[187] J. H. U. Daza, G. M. Righetto, M. V. Chaud, V. da Conceição Amaro Martins, I. Lopes Baratella da Cunha Camargo, and A. Maria de Guzzi Plepis, "PVA/anionic collagen membranes as drug carriers of ciprofloxacin hydrochloride with sustained antibacterial activity and potential use in the treatment of ulcerative keratitis," *J Biomater Appl*, vol. 35, no. 3, pp. 301–312, Sep. 2020, doi: 10.1177/0885328220931733.

[188] Z. Lei, H. Liang, W. Sun, Y. Chen, Z. Huang, and B. Yu, "A biodegradable PVA coating constructed on the surface of the implant for preventing bacterial colonization and biofilm formation," *J Orthop Surg Res*, vol. 19, no. 1, p. 175, Mar. 2024, doi: 10.1186/s13018-024-04662-7.

[189] J. Yang, W. Bao, P. Jaumaux, S. Zhang, C. Wang, and G. Wang, "MXene-Based Composites: Synthesis and Applications in Rechargeable Batteries and Supercapacitors," *Adv Mater Interfaces*, vol. 6, no. 8, Apr. 2019, doi: 10.1002/admi.201802004.

[190] X. Lin *et al.*, "Fascinating MXene nanomaterials: emerging opportunities in the biomedical field," *Biomater Sci*, vol. 9, no. 16, pp. 5437–5471, 2021, doi: 10.1039/D1BM00526J.

[191] G. A. Asaro *et al.*, "MXene functionalized collagen biomaterials for cardiac tissue engineering driving iPSC-derived cardiomyocyte maturation," *NPJ 2D Mater Appl*, vol. 7, no. 1, p. 44, Jun. 2023, doi: 10.1038/s41699-023-00409-w.

[192] M. Solazzo, F. J. O'Brien, V. Nicolosi, and M. G. Monaghan, "The rationale and emergence of electroconductive biomaterial scaffolds in cardiac tissue engineering," *APL Bioeng*, vol. 3, no. 4, Dec. 2019, doi: 10.1063/1.5116579.

[193] S. Malik, S. Subramanian, T. Hussain, A. Nazir, and S. Ramakrishna, "Electrosprayed Nanoparticles as Drug Delivery Systems for Biomedical Applications," *Curr Pharm Des*, vol. 28, no. 5, pp. 368–379, Feb. 2022, doi: 10.2174/1381612827666210929114621.

[194] K. Sudesh, Y.-F. Lee, N. Sridewi, and S. Ramanathan, "The Influence of Electrospinning Parameters and Drug Loading on Polyhydroxyalkanoate (PHA) Nanofibers for Drug Delivery," *Int J Biotechnol Wellness Ind*, vol. 4, no. 4, pp. 103–113, Jan. 2016, doi: 10.6000/1927-3037.2015.04.04.1.

[195] Z. Cao *et al.*, "Amino-Modified Poly (l–lactic Acid) Nanofibers Enable pH-Stimulated Drug Release and NIR Real-Time Detection," *ChemNanoMat*, vol. 8, no. 2, Feb. 2022, doi: 10.1002/cnma.202100461.

[196] K. Adibkia, S. Yaqoubi, and S. M. Dizaj, "Pharmaceutical and Medical Applications of Nanofibers," 2017, pp. 338–363. doi: 10.4018/978-1-5225-0751-2.ch013.

[197] G. Agrawal and R. Agrawal, "Functional Microgels: Recent Advances in Their Biomedical Applications," *Small*, vol. 14, no. 39, Sep. 2018, doi: 10.1002/smll.201801724.

AUTHOR'S PUBLICATIONS

ARTICLE

- **Renkler, NZ**, Ud Din Babar, Z, Barra, M, Cruz Maya, I, De Santis, R, Girolamo, Marelli, M, Ferretti, AM, Zaheer, A, Iannotti, V, Guarino,V. «Optimizing Electrospun PVA Fibers with MXene Integration as biointerfaces for biosensing applications» (Accepted for publication) DOI: 10.1002/mame.202400433
- **Renkler, N.Z.**, Scialla, S., Russo, T., D'Amora, U., Cruz-Maya, I., De Santis, R., Guarino, V.* "Micro- and Nanostructured Fibrous Composites via Electro-Fluid Dynamics: Design and Applications for Brain." Pharmaceutics, 2024, 16, 134 https://doi.org/10.3390/pharmaceutics16010134
- Cruz-Maya I, Schiavone C, Ferraro R, **Renkler NZ**, Caserta S, Guarino V. "Designing Advanced Drug Delivery Systems: Core-Shell Alginate Particles through Electro-Fluid Dynamic Atomization." Pharmaceutics. 2024; 16(2):193. https://doi.org/10.3390/pharmaceutics16020193
- **Renkler, N.Z.**, Cruz Maya, I., Guarino, V. "Optimization of Polyvinyl Alcohol-Based Electrospun Fibers with Bioactive or Electroconductive Phases for Tissue-Engineered Scaffolds." Fibers 2023, 11, 85. https://doi.org/10.3390/fib11100085
- **Renkler, N.Z.**, Cruz-Maya, I., Bonadies, I., Guarino, V.* "Electro Fluid Dynamics: A Route to Design Polymers and Composites for Biomedical and Bio-Sustainable Applications" Polymers, 14, 4249, 2022 https://doi.org/10.3390/polym14194249

BOOK CHAPTER

- **Renkler, N. Z.**, I. Cruz-Maya, V. Guarino «Electro Fluid Dynamic Technologies to Engineer 3D Matrices for Glial Cells in Brain» Glial Engineering and Glial Interfaces: Targeting the Role of Astrocytes and Other Glial Cells in Brain Function and Dysfunctions (Submitted)

- Cruz-Maya, I., **Renkler, NZ**., Guarino, V. "Chapter 13: Ionotropically cross-linked polymeric beads for drug delivery", Ionotropic Cross-Linking of Biopolymers: Applications in Drug Delivery Ed. A.K. Nayak, S. Hasnain, Elsevier, 2024 https://doi.org/10.1016/B978-0-323-96116-5.00020-X

INTERNATIONAL COMMUNICATIONS

- Optimizing Electrospun PVA Fibers with MXene Integration as Biointerfaces for Biosensing Applications. 3rd BioCube Workshop and Winter School in Biophotonics, Bioelectronics and Biomechanics, Sestriere, Italy, 2024 (Poster)
- Optimization of PVA based Nanofibers via Green Electrospinning for Biomedical Applications. The 6th European Symposium on Electrohydrodynamic Atomization and Electrospinning, Krakow, Poland, 2023 (Oral Presentation)
- Core Shell Alginate Particles: Design and Modeling for Drug Delivery. 26th International Bioengineering Congress, Ankara, Turkey, 2022 (Poster).
- PVA Based Scaffolds via Green Electrospinning for Biomedical Applications. 26th International Bioengineering Congress, Ankara, Turkey, 2022 (Poster).
- Preparation of PVA based Nanofibers for in vitro cell interactions. The 5th European Symposium on Electrohydrodynamic Atomization and Electrospinning, Naples, Italy, 2022 (Poster)

PROJECT

- Horizon 2020 Marie Skłodowska-Curie Actions – ASTROTECH: Disruptive materials, technologies & approaches to unravel the role of Astrocytes in brain function and dysfunction: towards to Glial interfaces (Role: Early Stage Researcher)
  My primary contributions involved designing and producing electrospun nanofiber scaffolds tailored to mimic the extracellular matrix environment, enabling a deeper understanding of astrocyte behavior. I have optimized polymer blends such as PVA and gelatin to meet the mechanical and biological requirements for astrocyte studies. Furthermore, I have conducted in

vitro experiments to evaluate biocompatibility and to study astrocyte-material interactions, which are essential for advancing glial interface technologies.